$7

QEX

September/October 2017

www.arrl.org

QEX

A Forum for Communications Experimenters

Issue No. 304

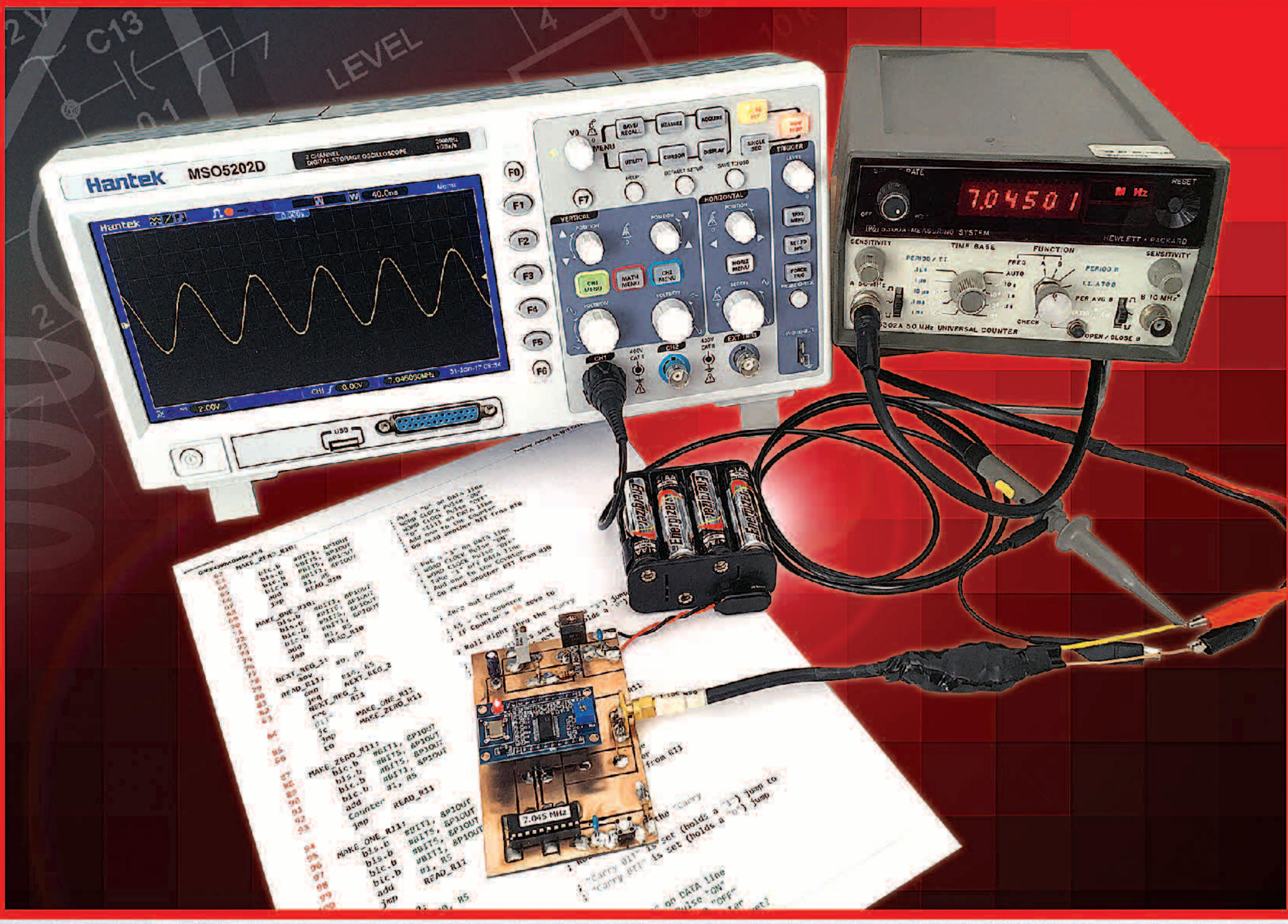

AE7AX generates a perfect sine wave using machine code to program a Direct Digital Synthesizer.

ARRL
The national association for
AMATEUR RADIO™
225 Main Street
Newington, CT USA 06111-1494

New

APRS® / D-STAR®

TH-D74A 144/220/430 MHz Tribander

Introducing the TH-D74A for the ultimate in APRS and D-STAR performance. KENWOOD has already garnered an enviable reputation with the TH-D72A handheld APRS amateur radio transceiver. And now it has raised the bar even further with the new TH-D74A, adding support for D-STAR, the digital voice & data protocol developed by the JARL, and enabling simultaneous APRS and D-STAR operation – an industry first.

- APRS compliance using packet communication to exchange real-time GPS position information and messages
- Compliant with digital/voice mode D-STAR digital amateur radio networks
- Built-in high performance GPS unit with Auto Clock Setting
- Wide-band and multi-mode reception
- 1.74" (240 x 180 pixel) Transflective color TFT display
- IF Filtering for improved SSB/CW/AM reception
- High performance DSP-based audio processing & voice recording
- Compliant with Bluetooth, microSD & Micro-USB standards
- External Decode function (PC Decode 12kHz IF Output, BW:15 kHz)
- Free software for Memory and Frequency Control Program
- Data Import / Export (Digital Repeater List, Call sign, Memory Channel)
- Four TX Power selections (5/2/0.5/0.05 W)
- Dust and Water resistant IP54/55 standards

APRS (The Automatic Packet Reporting System) is a registered American trademark of WB4APR (Mr. Bob Bruninga).
D-Star is a digital radio protocol developed by JARL (Japan Amateur Radio League).

KENWOOD

Customer Support/Distribution Customer Support:
(310) 639-4200 Fax: (310) 537-8235

www.kenwood.com/usa

JQA-1205 091
ISO9001 Registered
Professional Systems Business Group
JVCKENWOOD Corporation

ADS#29016

QEX (ISSN: 0886-8093) is published bimonthly in January, March, May, July, September, and November by the American Radio Relay League, 225 Main Street, Newington, CT 06111-1494. Periodicals postage paid at Hartford, CT and at additional mailing offices.

POSTMASTER: Send address changes to: QEX, 225 Main St, Newington, CT 06111-1494
Issue No 304

Publisher
American Radio Relay League

Kazimierz "Kai" Siwiak, KE4PT
Editor

Lori Weinberg, KB1EIB
Assistant Editor

Zack Lau, W1VT
Ray Mack, W5IFS
Contributing Editors

Production Department

Steve Ford, WB8IMY
Publications Manager

Michelle Bloom, WB1ENT
Production Supervisor

Sue Fagan, KB1OKW
Graphic Design Supervisor

David Pingree, N1NAS
Senior Technical Illustrator

Brian Washing
Technical Illustrator

Advertising Information Contact:

Janet L. Rocco, W1JLR
Business Services
860-594-0203 – Direct
800-243-7768 – ARRL
860-594-4285 – Fax

Circulation Department

Cathy Stepina, *QEX Circulation*

Offices

225 Main St, Newington, CT 06111-1494 USA
Telephone: 860-594-0200
Fax: 860-594-0259 (24 hour direct line)
e-mail: **qex@arrl.org**

Subscription rate for 6 issues:

In the US: $29;

US by First Class Mail: $40;

International and Canada by Airmail: $35

Members are asked to include their membership control number or a label from their QST when applying.

In order to ensure prompt delivery, we ask that you periodically check the address information on your mailing label. If you find any inaccuracies, please contact the Circulation Department immediately. Thank you for your assistance.

Copyright © 2017 by the American Radio Relay League Inc. For permission to quote or reprint material from *QEX* or any ARRL publication, send a written request including the issue date (or book title), article, page numbers and a description of where you intend to use the reprinted material. Send the request to the office of the Publications Manager (**permission@arrl.org**).

About the Cover

James L. Kretzschmar, AE7AX, uses the Texas Instruments MSP430 LaunchPad development kit to generate his own machine code program to drive the AD9850 Signal Generator module. To accomplish this task, he uses Code Composer, the Texas Instruments online Integrated Development Environment. The project was motivated by the need for a stable and precise way to generate a frequency for experimental projects in both the VLF and low HF regions of the radio spectrum.

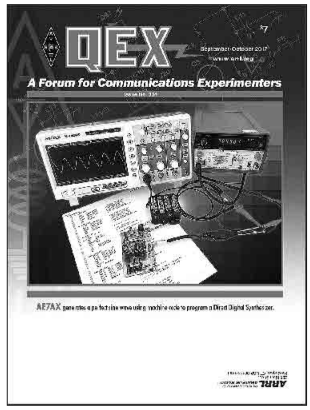

In This Issue

Features

Index of Advertisers

The American Radio Relay League

The American Radio Relay League, Inc, is a noncommercial association of radio amateurs, organized for the promotion of interest in Amateur Radio communication and experimentation, for the establishment of networks to provide communications in the event of disasters or other emergencies, for the advancement of the radio art and of the public welfare, for the representation of the radio amateur in legislative matters, and for the maintenance of fraternalism and a high standard of conduct.

ARRL is an incorporated association without capital stock chartered under the laws of the state of Connecticut, and is an exempt organization under Section 501(c)(3) of the Internal Revenue Code of 1986. Its affairs are governed by a Board of Directors, whose voting members are elected every three years by the general membership. The officers are elected or appointed by the Directors. The League is noncommercial, and no one who could gain financially from the shaping of its affairs is eligible for membership on its Board.

"Of, by, and for the radio amateur," ARRL numbers within its ranks the vast majority of active amateurs in the nation and has a proud history of achievement as the standard-bearer in amateur affairs.

A *bona fide* interest in Amateur Radio is the only essential qualification of membership; an Amateur Radio license is not a prerequisite, although full voting membership is granted only to licensed amateurs in the US.

Membership inquiries and general correspondence should be addressed to the administrative headquarters:

ARRL
225 Main Street
Newington, CT 06111 USA
Telephone: 860-594-0200
FAX: 860-594-0259 (24-hour direct line)

Officers

President: Rick Roderick, K5UR
PO Box 1463, Little Rock, AR 72203

Chief Executive Officer: Tom Gallagher, NY2RF

The purpose of *QEX* is to:

1) provide a medium for the exchange of ideas and information among Amateur Radio experimenters,

2) document advanced technical work in the Amateur Radio field, and

3) support efforts to advance the state of the Amateur Radio art.

All correspondence concerning *QEX* should be addressed to the American Radio Relay League, 225 Main Street, Newington, CT 06111 USA. Envelopes containing manuscripts and letters for publication in *QEX* should be marked Editor, *QEX*.

Both theoretical and practical technical articles are welcomed. Manuscripts should be submitted in word-processor format, if possible. We can redraw any figures as long as their content is clear. Photos should be glossy, color or black-and-white prints of at least the size they are to appear in *QEX* or high-resolution digital images (300 dots per inch or higher at the printed size). Further information for authors can be found on the Web at **www.arrl.org/qex/** or by e-mail to **qex@arrl.org**.

Any opinions expressed in *QEX* are those of the authors, not necessarily those of the Editor or the League. While we strive to ensure all material is technically correct, authors are expected to defend their own assertions. Products mentioned are included for your information only; no endorsement is implied. Readers are cautioned to verify the availability of products before sending money to vendors.

Kazimierz "Kai" Siwiak, KE4PT

Perspectives

The Power of the Basic SDR System

We identified the basic SDR system in this column as comprising some form of RF front end, followed by conversion between the analog and digital realms, along with a general purpose personal computer (PC). The SD or *software defined* part of the system is the Amateur Radio communications software that operates on the PC, producing a wide range of different communications protocols, or "waveforms" that usually are not native to the transceiver used as the RF front end. To be sure, SDR receiver and transmitter platform architectures continue to migrate the boundary between the analog and digital realm closer to the antenna — but even those platforms also require, and benefit from, the development of new PC-based waveforms or modes.

The general purpose personal computer was once called the first consumer product sold without a specific consumer purpose. Added software defined its purpose. Our basic SDR system hardware might remain constant, but it is the added operating software that defines an evolving, clever, highly capable and innovative amateur communications purpose. As a result, our Amateur Radio communications capabilities have grown dramatically without a need to change the basic hardware. Waveforms have and will continue to be designed and fine-tuned for specialized and difficult propagation paths such a Earth-Moon-Earth, meteor scatter, or just to generally increase the path link margin.

Watch these pages for additional modulation waveforms, and for further SDR evolution.

In This Issue

Our *QEX* authors touch upon a wide variety of Amateur Radio topics. These are at the top of the queue.

Steven J. Franke, K9AN, and Joseph H. Taylor, K1JT, describe the modulation, message structure, channel coding, and special operational features of the new meteor-scatter mode implemented in *WSJT-X*.

Robert J. Zavrel, W7SX, explains field-strength and power combining in various configurations of dipoles and dipole arrays.

James L. Kretzschmar, AE7AX, gets precision frequency control with assembly code.

David Birnbaum, K2LYV, shows how to calculate the LC trap values given the physical size of the antenna and two desired resonant frequencies.

John E. R. White, VA7JW, presents experimental results of a water seepage into the PL-259 connector.

Ed Callaway, N4II and Kai Siwiak, KE4PT, comment on the signal to noise ratio and polarization at HF considering atmospheric noise.

Keep the full-length *QEX* articles flowing in, but if a full length article is not your aspiration, share a brief **Technical Note** that is perhaps several hundred words long plus a figure or two. Expand on another author's work and add to the Amateur Radio *institutional memory* with your technical observation. Let us know that your submission is intended as a **Note**.

QEX is edited by Kazimierz "Kai" Siwiak, KE4PT, (**ksiwiak@arrl.org**) and is published bimonthly. *QEX* is a forum for the free exchange of ideas among communications experimenters. The content is driven by you, the reader and prospective author. The subscription rate (6 issues per year in the United States is $29. First Class delivery in the US is available at an annual rate of $40. For international subscribers, including those in Canada and Mexico, *QEX* can be delivered by airmail for $35 annually. Subscribe today at **www.arrl.org/qex**.

Would you like to write for *QEX*? We pay $50 per published page for articles and Technical Notes. Get more information and an Author Guide at **www.arrl.org/qex-author-guide**. If you prefer postal mail, send a business-size self-addressed, stamped (US postage) envelope to: *QEX* Author Guide, c/o Maty Weinberg, ARRL, 225 Main St, Newington, CT 06111.

73,

Kazimierz "Kai" Siwiak, KE4PT

James L. Kretzschmar, AE7AX

7420 Huntz Drive, Cheyenne, WY 82009, USA: **jlkwy@bresnan.net**

Programming the DDS AD9850 Signal Generator Module with the Texas Instruments MSP430 LaunchPad

Precision frequency control with assembly code.

The AD9850 Signal Generator module has been available for several years and there are many online sites that provide program code. However, using these pre-packaged programs does not give you the flexibility and control that can be realized by developing your own code. This article describes how to achieve this control by using the Texas Instruments MSP430 LaunchPad to drive the AD9850 Signal Generator module. To accomplish this task, we will be using the Texas Instruments free online IDE (Integrated Development Environment) called Code Composer.[1] To accelerate the process of learning a new software application, a step-by-step guide can be found in *QEXfiles* web page.[2] The inspiration for this project was the need for a stable and precise way to generate a frequency for experimental projects in both the VLF regions of the radio spectrum and the 40 meter band.

First, the features of the MSP430 LaunchPad and AD9850 Signal Generator module are described followed by a discussion on the documentation. Next is a detailed discussion on configuring the AD9850 module and how to calculate the Frequency Number that will be entered into the module. The next section provides a detailed discussion on the mechanics of the Assembly code program. Bringing it all together are the details for building a fixed frequency signal generator for 7.045 MHz. The frequency can easily be modified to fit your needs.

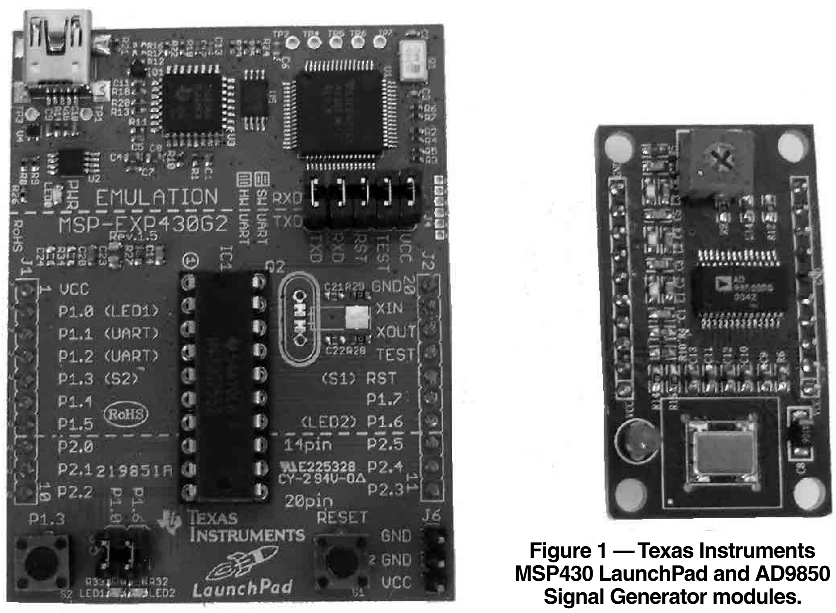

Figure 1 — Texas Instruments MSP430 LaunchPad and AD9850 Signal Generator modules.

Texas Instruments MSP430 LaunchPad

The MSP430 LaunchPad is an easy-to-use development board for the low-power and low-cost MSP430G2x family of microcontrollers and is available from Texas Instruments and other distributors for $10 (see Figure 1). It has on-board emulation for programming and debugging, and includes a 14/20-pin DIP socket, two on-board tactile switches and two LEDs for easy initial experimentation. The MSP430 LaunchPad comes with two MSP430 microcontrollers, the MSP430G2553 and MSP430G2452. We will use the MSP430G2553 which has 16 kB Flash memory, 512 B RAM, and a CPU speed of 16 MHz. In addition, peripherals incorporated into the microcontroller include an 8 channel 10-bit ADC (Analog-to-Digital Converter), two timers, and serial communication capabilities (UART, I2C and SPI). Useful features of the LaunchPad are that it can program a variety of the MSP430 family of microcontrollers and the chip can be removed from the LaunchPad board and incorporated into a project. Detailed documentation for the microcontrollers included with the MSP430 LaunchPad is available from the Texas Instruments web page.[3]

DDS AD9850 Signal Generator Module

The AD9850 Signal Generator module provides a single frequency output in the range of 0-40 MHz and is available from several online sources for about $16. (see Figure 1). The frequency is defined by a 40-bit Tuning Word that can be sent to the module in either serial or parallel format. The signal phase is controlled by bits 34-39 of the Tuning Word. The module has an onboard 125 MHz reference clock and can be powered by a 5.0 or 3.3 V power supply. For this project, the 3.3 V supply available from the MSP430 LaunchPad will be used, the 40-bit Tuning Word will be entered in serial format, and bits 34-39 will be set to "0". Setting these five bits to "0" produces no change in the phase of the signal. Please note, if two of these modules were to be used for mixing same frequency signal sources that are out of phase, they must both operate from the same reference clock.

Documentation

Documentation for the AD9850 Signal Generator module is available online and does provide a schematic diagram which is useful when configuring the AD9850 module for entry of data in serial mode.[4] The Analog Devices AD9850 datasheet is comprehensive and the figures and diagrams were very helpful in the development of the Assembly program for the MSP430G2553 microcontroller.

After studying the Analog Devices AD9850 datasheet two things became apparent. First, it is necessary to enter a 40-bit Serial-Load Enable Word to establish serial mode operation (this will be discussed in detail in the Assembly Code Program section). Second, in the tables, the terms "W0 - W39" actually refer to "bits" instead of "Words".

AD9850 Configurations

When setting up for serial mode the Analog Devices AD9850 datasheet (page 12, Figure 23) shows that pins 3 and 4 of the AD9850 chip must be tied to the supply voltage, and pin 2 of the AD9850 chip must be grounded. On the AD9850 module pins 3 and 4 are wired to the supply voltage, however, pin 2 is connected to pin D2. Thus, pin D2 of the AD9850 module needs to be grounded for serial operation.

Referring to the Analog Devices AD9850 datasheet (page 12, Figure 22 and Figure 24) there are 3 lines necessary to operate the AD9850. The logic analyzer pictures (see Figures 2, 3, and 4) show these three lines and will be helpful in understanding how data is inputted into the AD9850 module. These three lines are:

1 – DATA line – This is where the 40-bit Serial-Load Enable Word and 40-bit Tuning Word are input into the device.

2 – W_CLK line – (Word Clock line). The W_CLK line is pulsed each time one of the 40 bits of either the Serial-Load Enable Word or the Tuning Word is placed on the DATA line. This line is also pulsed once at the beginning of Serial-Load Enable Word word load sequence.

3 – FQ_UD line – This is the frequency update line. When the 40-bit Serial-Load

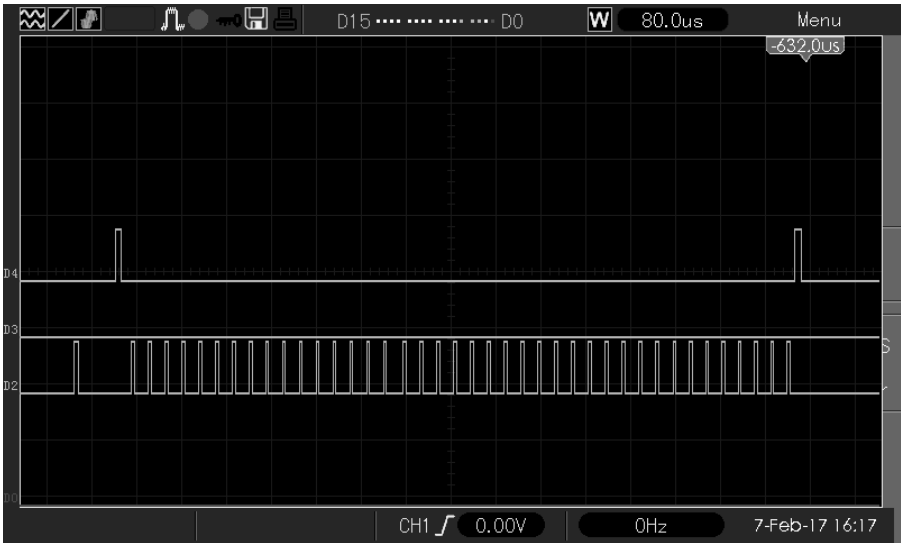

Figure 2 — Logic analyzer picture of 40-bit serial-load enable word, bit-0 on the left and bit-39 on the right. W_CLK line is on the bottom, DATA line in the middle, and FQ_UD line on the top. Note that the DATA line is all "0"s.

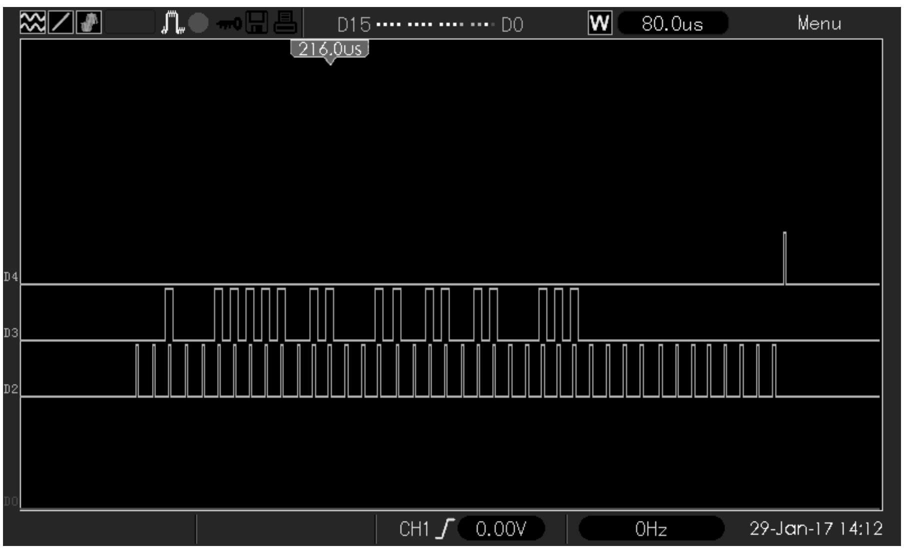

Figure 3 — Logic Analyzer picture of the 40-bit Tuning Word for 7.045 MHz. bit-0 is on the left and bit-39 is on the right. W_CLK line is on the bottom, DATA line in the middle, and FQ_UD line on the top.

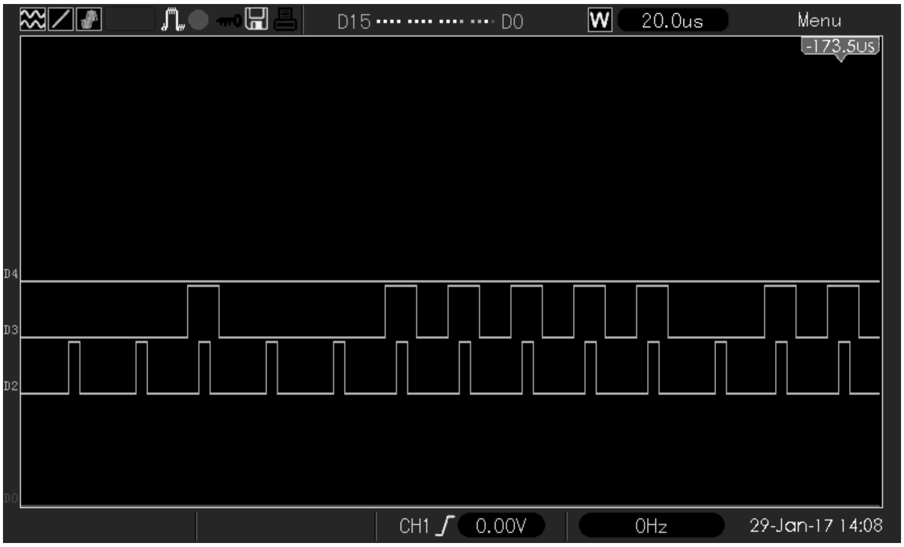

Figure 4 — Enlarged view of the logic analyzer picture of bit-0 (left) through bit-12 (right) of the 40-bit Tuning Word for 7.045 MHz. The timing relationship between the W_CLK line and the bits on the DATA line is clearly seen.

Enable Word is loaded, this line is pulsed at the beginning of the load and at the end of the load.

The Analog Devices AD9850 datasheet (page 3, Timing Characteristics) notes that when any one of these lines is brought "High" it must remain in that state for a minimum of 3.5 ns. In this project we are using the MSP430G2553 microcontroller default CPU clock speed of 1 MHz, which provide pulses well above the minimum requirement.

Table 1
The 40-bit Tuning Word

PHASE + CONTROL	*FREQUENCY NUMBER*
bits (39-35)+(34-32)	bits (31-0)

Calculating the 40-bit Tuning Word

The 40-bit Tuning Word is composed of two parts. The first 32 bits (0-31) are the Frequency Number, and the last 8 bits are the three control bits (32-34) and the five phase selection bits (35-39). The three control bits will be discussed in the next section and all will be "0". The five phase selection bits, as explained earlier, are all set to "0". Table 1 shows a generic pictorial of the 40-bit Tuning Word. The numbers in parenthesis are the bits with the most significant bit (MSB) on the left and the least significant bit (LSB) on the right.

The calculation for the Frequency Number is accomplished outside of the Assembly program and is first calculated in decimal (base 10), then converted into binary (base 2). Calculate the 32-bit Frequency Number according to the AD9850 data sheet.

Table 2
Memory storage for the 40-bit Serial-Load Enable Word

Register 8	*Register 7*	*Register 6*
0000 0000 bits (39-32) (Decimal = 0)	0000 0000 0000 0000 bits (31-16) (Decimal = 0)	0000 0000 0000 0000 bits (15-0) (Decimal = 0)

Table 3
Assembly program lines that store numbers in Registers 6 – 8

mov #0, R6	; Moves "0" into Register 6 ; bits (0-15) of the 40-bit Serial-Load Enable Word
mov #0, R7	; Moves "0" into Register 7 ; bits (16-31) of the 40-bit Serial-Load Enable Word
mov #0, R8	; Moves "0" into Register 8 ; bits (32-39) of the 40-bit Serial-Load Enable Word

$$\text{Frequency Number} = \frac{\text{Frequency to be programmed}}{\text{Reference frequency}} \times 2^{32}$$

$$\text{Frequency Number} = \frac{7.045 \text{ MHz}}{125.000 \text{ MHz}} \times 4,294,967,296$$

$$= 242,064,356$$

Convert the 32-bit Frequency Number into a binary number with the help of an online decimal/binary/hexadecimal calculator.[5] The Frequency Number of 242,064,356 is represented by the 28-bit binary number binary sequence,

1110011011011001101111100100

or when parsed into 4-bit segments,

1110 0110 1101 1001 1011 1110 0100.

Since we need a 32 bit Frequency Number and this converted number for 7.045 MHz has only 28 positions filled (bits 0 to bit 27, right to left), we must add four 0 bits in positions 28 to 31 on the left,

0000 1110 0110 1101 1001

1011 1110 0100, is now a 32 bit sequence.

The Frequency Number is now ready for manipulation so it can be inserted into the assembly program.

Assembly Code Program

To understand how both the 40-bit Serial-Enable Word and the 40-bit Tuning Word are loaded into the AD9850 it is best to follow along with the assembly code program that can be found in the *QEXfiles* web page. The program is comprised of three parts.

1 – Initialization

(a) The pins of the microcontroller are defined as to which ones will be used for the DATA line, W_CLK line, and the FQ_UD line.

(b) Memory storage for the 40-bit Serial-Load Enable Word. The program code uses three of the twelve 16-bit general purpose registers of the MSP430G2553 microcontroller to store the 40-bit Serial-Load Enable Word. Bits (39-32) are stored in Register 8, bits (31-16) in Register 7, and bits (15-0) in Register 6, as shown Table 2, according to the code shown in Table 3. Following the Analog Devices AD9850 datasheet (see page 12, Figure 22), bits 32, 33, and 34 of the 40-bit Serial-Load Enable Word must all be "0". To keep the rest of the 40-bit Serial-Load Enable Word uncomplicated, the remaining 37 bits were all made "0".

(c) Memory storage for the 40-bit Tuning Word (Table 4). Another 3 registers are used to store the 40-bit Tuning Word. Bits (39-32) are stored in Register 12, bits (31-16) in Register 11, and bits (15-0) in Register 10.

The 32-bit Frequency Number is divided into two 16-bit sections and stored in Register 10 and Register 11. Register 12 is also a 16-bit register, however, the Assembly code (Table 5) is written to use only the first 8 bits that will hold the Phase and Control information.

2 – Development of the "40-bit Serial-Load Enable Word"

See Figure 2.

(a) W_CLK line is pulsed once

(b) FQ_UD line is pulsed once

(c) The process for shifting data out of Registers 6, 7, and 8 onto the AD9850 DATA line for the Serial-Load Enable Word uses the Assembly instruction RRC (Roll Right through the Carry bit). Starting with Register 6, as each bit is shifted out of the register to the right, it is placed in the "Carry bit" and tested as to whether it is a "1" or a "0". The program then branches accordingly to make a "1" (DATA line brought "High"), or a "0" (DATA line brought "Low").

(d) While the "1" or "0" is on the DATA line, the W_CLK line is pulsed

(e) The "1" or "0" is then removed from the DATA line, and the next bit is shifted to the right with the RRC instruction and tested.

(f) After all 16 bits have been shifted out of Register 6, then Registers 7 and 8 are handled in the same way. A counter keeps track of when 40 bits have been placed on the DATA line.

(g) FQ_UD line is pulsed once.

3 – Development of the "40-bit Tuning Word"

See Figure 3 and Figure 4.

(a) The process for shifting data out of Registers 10, 11, and 12 into the AD9850. Starting with Register 10, as each bit is shifted out of the register to the right, it is placed in the "Carry bit" and tested as to whether it is a "1" or "0". The program then branches accordingly to make a "1" (DATA line brought "High"), or a "0" (DATA line brought "Low").

(b) While the "1" or "0" is on the DATA line the W_CLK line is pulsed.

(c) The "1" or "0" is then removed from the DATA line, and the next bit is shifted to the right with the RRC instruction and tested.

(d) After all 16 bits have been shifted out of Register 10, then Registers 11 and 12 are handled in the same way. A counter keeps track of when 40 bits have been placed on the DATA line.

(e) FQ_UD line is pulsed once.

Table 4
Memory storage for the 40-bit Tuning Word

Register 12	*Register 11*	*Register 10*
0000 0000	0000 1110 0110 1101	1101 1011 1110 0100
bits (39-32)	bits (31-16)	bits (15-0)
(Decimal = 0)	(Decimal = 3693)	(Decimal = 39908)

Table 5
Assembly program lines that store numbers in Registers 10 – 12

```
mov #39908, R10          ; Moves "39908" into Register 10
                         ; bits (0-15) of 40-bit Tuning Word
mov #3693, R11           ; Moves "3693" into Register 11
                         ; bits (16-31) of 40-bit Tuning Word
mov #0, R12              ; Moves "0" into Register 12
                         ; bits (32-39) of 40-bit Tuning Word
```

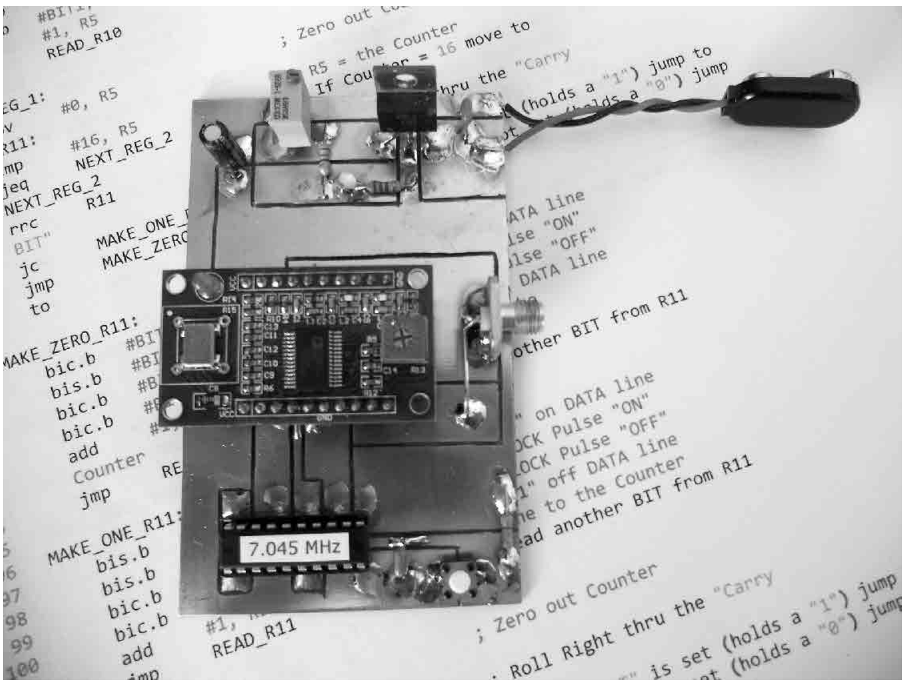

Figure 5 — Fixed frequency signal generator showing the MSP430G2553 microcontroller, AD9850 module,

Fixed Frequency Signal Generator

The Fixed Frequency Signal Generator is comprised of three sections, (1) the microcontroller, (2) the AD9850 module, and (3) a voltage regulator (see Figure 5 and Figure 6). The board template and parts placement diagram can be found in *QEXfiles* web page. Following the schematic diagram of the MSP430 LaunchPad, one tactile switch was connected from pin 16 of the microcontroller to ground for a reset of the MSP430G2553 if needed. To mount the AD9850 module, two 10-pin female header receptacles were used. On both the 20-pin microcontroller socket and the header receptacles, the unused pins were pulled out to make the board design and soldering easier. Pins 10 and 11 of the microcontroller socket have no electrical connections and are used solely to anchor the IC socket. The LM317T variable voltage regulator was chosen so that it could be set to 3.3 V, the same voltage available on the MSP430 LaunchPad.

Once the MSP430G2553 microcontroller is programmed it is removed from the LaunchPad and placed in the IC socket on the board. Applying power initiates the code routine in the microcontroller, and the data is delivered to the AD9850 module, which outputs a very stable and precise sine wave (see Figure 7). In the development of this project two observations were made. First, the frequency observed on the measurement equipment is dependent upon the accuracy of the reference oscillators on the AD9850 module and in the test equipment. This

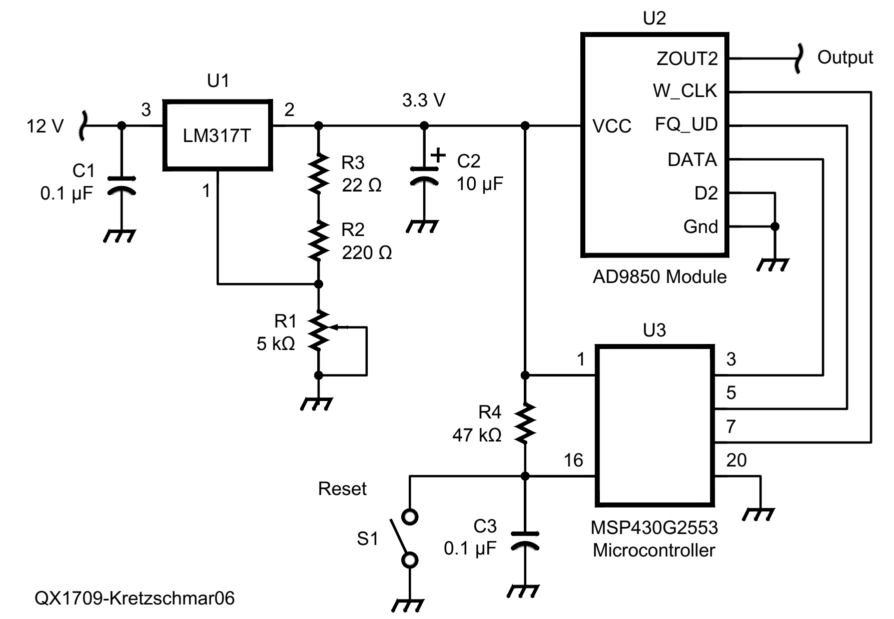

Figure 6 — Schematic diagram of the fixed frequency signal generator.

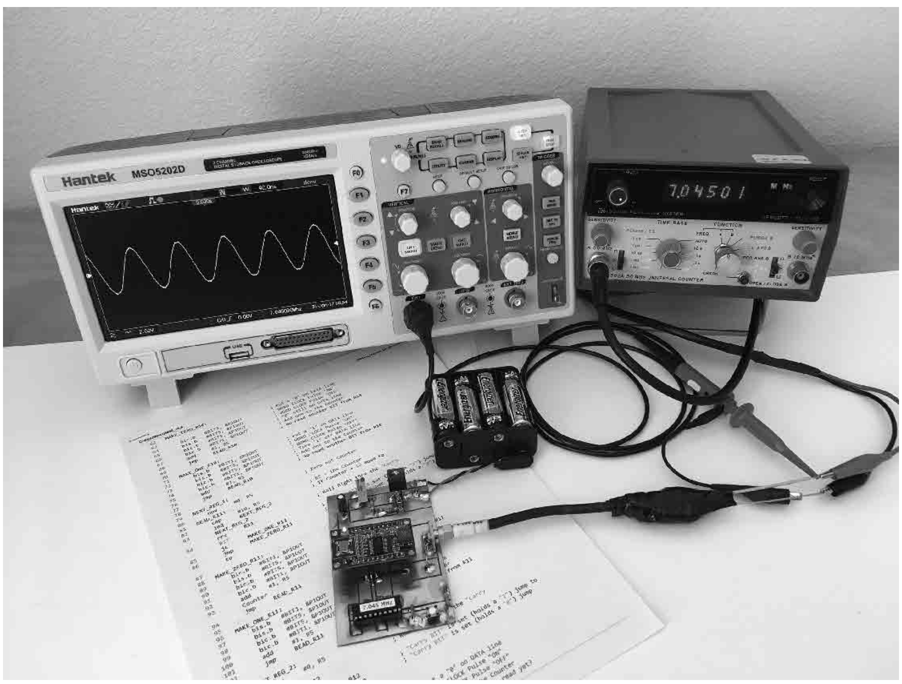

Figure 7 — Output of fixed frequency signal generator at 7.045 MHz.

will most likely result in the observed frequency to be a few hertz different from the calculated frequency. Second, during initial testing, the jumper wires between the MSP430 LaunchPad and the AD9850 module occasionally picked up stray signals (i.e., static) causing the code to not load properly. On the final board stray signal pick up was not a problem.

Summary

Writing your own program in assembly code for the Texas Instruments MSP430G2553 microcontroller allows you to precisely control the frequency output of the AD9850 DDS Signal Generator module. Possible applications include a frequency standard, the first stage of a beacon transmitter, or a way to generate a precise frequency in one of the proposed VLF Amateur Radio bands. Whatever your frequency generation application may require, this project will provide a stable and precise signal. Enjoy experimenting and have fun.

James Kretzschmar, AE7AX, was first licensed in 1972 as a Novice and now holds an Amateur Extra class license. He retired from the US Air Force in 2004 after a 25 year career as a general dentist. He currently works part time in the Oral Surgery department at the Alaska Native Medical Center in Anchorage, Alaska. James received a BA degree in chemistry from Texas Christian University, masters degree in Basic Science from the University of Colorado, and Doctor of Dental Surgery degree from Baylor College of Dentistry. In the past two years he has taken courses in the Electrical and Computer Engineering department at the University of Wyoming on Microcontrollers and Biomedical Instrumentation. He was awarded the "Best Humanitarian Impact" category prize in the 2016 Texas Instruments Innovation Challenge competition for his entry, "Futuristic Energy Saving Lighting System, Color Influenced Temperature Perception". His project involved temperature input to a microcontroller for regulation of RGB LED room lighting. James is an ARRL member and enjoys all aspects of electronics, homebrew projects, 40 meter CW operating, and bicycling.

Notes

[1]Download of Code Composer from Texas Instruments, **www.ti.com/lsds/ti/tools-software/ccs.page**.
[2]**arrl.org/qexfiles**.
[3]**processors.wiki.ti.com/index.php/Getting_Started_with_the_MSP430_LaunchPad_Workshop**.
[4]**www.analog.com/media/en/technical-documentation/data-sheets/AD9850.pdf**.
[5]Online calculator, **https://www.mathisfun/binary-decimal-hexadecimal-converter**.

Steven J. Franke, K9AN
3314 E. Anthony Dr., Urbana, IL 61802; **k9an@arrl.net**

Joseph H. Taylor, K1JT
272 Hartley Ave, Princeton, NJ 08540; **k1jt@arrl.net**

The MSK144 Protocol for Meteor-Scatter Communication

Here's a full description of the modulation, message structure, channel coding, and special operational features of the new meteor-scatter mode implemented in WSJT-X.

Meteor-scatter communication was first described[1] in the pages of *QST* in 1953 as a means for communicating on dead 15 and 20 m bands. Hams soon realized that even more impressive results could be obtained at 6 and 2 m, where background noise levels are much lower and useful low-elevation gain is obtainable with relatively modest antennas. Early meteor-scatter (MS) contacts used CW and relied on relatively rare "blue whizzer" meteor trails that last several seconds or longer. Today we can use a fast digital mode with built-in error correction to make contacts on VHF bands any day of the year, out to 1300 miles or so, using meteor-induced "pings" shorter than 0.1 s — with no dependence on weather, solar activity, position of the moon, or fickle band openings.

European hams pioneered the use of high-speed CW (HSCW) in the 1960s and 1970s, using Morse code at speeds 10 to 40 characters per second (cps; 10 cps=120 WPM) to convey short messages using pings as short as several tenths of a second. Modified cassette tape recorders saved the received audio and played it back at low speed, for decoding by ear. By the late 1990s, personal computers were used to send and receive HSCW at speeds as high as 150 cps. Shelby Ennis, W8WN, described the state of the art in HSCW circa 2000 in *QST*.[2] Soon afterward K1JT introduced computer program *WSJT*[3] with the FSK441 protocol, the first amateur digital mode designed specifically to communicate with the shortest and most frequent meteor pings. FSK441 uses 4-tone frequency-shift-keying and noncoherent demodulation. Its character transmission rate is 147 cps, and it provides reliable copy for signals a few dB above the noise in a 2500 Hz bandwidth. Since 2001 hundreds of thousands of MS contacts have been made with FSK441 on the VHF bands, and some even as high as 432 MHz.

Today's computers are considerably more powerful than those of 2001. This rapid technology advance has enabled us to develop MSK144, a practical protocol for meteor scatter that uses bandwidth-efficient modulation and cutting-edge tools for forward error correction (FEC). When designing this protocol we gave high priority to considerations of transmission speed, sensitivity, and decoding efficiency. The final design choices for MSK144 are well matched to the nature of MS signals on the amateur VHF bands and the characteristics of today's amateur transceivers. The effective transmission rate of 250 cps makes good use of very short pings and can be shown to be a practical speed limit for the typical 2500 Hz bandwidth of amateur SSB transceivers. The generated MSK144 waveform ensures that decoders can use coherent demodulation and even coherent averaging over multiple message frames. Using these techniques, we find that some MSK144 signals can be decoded with signal-to-noise ratios as low as −8 dB in the standard 2500 Hz reference bandwidth. Following its public introduction in the summer of 2016, MSK144 has rapidly become the world-wide mode of choice for amateur MS contacts.

In this paper we present technical details of the MSK144 protocol and describe its motivation and underlying design philosophy. We begin by describing the modulation, frame structure, and error-control coding, paying particular attention to the spectrum and envelope shape of generated waveforms. We include on-the-air spectral measurements and the results of simulations that establish the decoding sensitivity and false-decode rate. We then present some details of the MSK144 decoder as implemented in the popular open-source computer program *WSJT-X*,[4] followed by some special operational features of the program in MSK144 mode. These features include semi-automated tools for convenient use of a standard MS calling frequency; a contest mode to facilitate exchange of required information in North American VHF contests; a special short-message format useful at 144 MHz and higher frequencies; and a tool for measuring and compensating frequency-dependent phase shifts in the receiver passband.

Modulation and Coding

MSK stands for *minimum shift keying*, a form of continuous-phase frequency-shift keying (FSK) with shift equal to half the baud rate. MSK144 uses *message frames* of 144 bits and modulation at tone frequencies 1000 and 2000 Hz to transmit *channel symbols* at keying rate of 2000 baud. The resulting audio waveform can be viewed as a form of offset quadrature phase-shift keying (OQPSK) with individual pulses shaped like the first half-period of a sine wave. Using this OQPSK viewpoint, the continuous-time representation of an MSK144 signal can be written as

$$s(t) = I(t)\cos\omega_c t - Q(t)\sin\omega_c t$$

where the waveforms $I(t)$ and $Q(t)$ are called the in-phase and quadrature components of the signal, respectively. In *WSJT-X* the MSK144 waveform is generated with carrier frequency $f_c = \omega_c / 2\pi = 1500$ Hz, and the resulting audio signal is transmitted as upper sideband by a standard single sideband (SSB) transmitter.

Example waveforms for $I(t)$ and $Q(t)$ in Figure 1 show how the in-phase and quadrature signals are created from half-sine pulses with 1 ms duration. Note that the $Q(t)$ waveform is shifted by half a symbol relative to $I(t)$; therefore half-symbols appear at the start and end of the $Q(t)$ waveform in this plot. Pulses with positive polarity represent bits with value 1, negative pulses represent 0. With the convention that bit indices begin at zero, even-numbered bits are sent on the *Q* channel, odd-numbered bits on the *I* channel. The waveform shown in Figure 1 represents the bit sequence 01100110101101010.

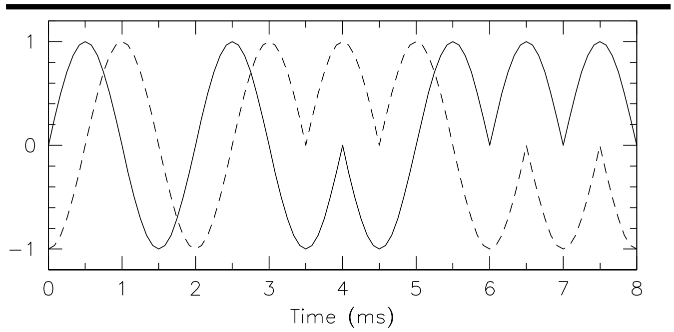

Figure 1 — Short segment of the in-phase, $I(t)$ (*solid curve*) and quadrature, $Q(t)$ (*dashed curve*) components of an MSK144 waveform. The in-phase waveform contains 8 contiguous half-sine pulses. The quadrature waveform is offset by half of a pulse. The offset and half-sine shaping ensures that the envelope of the MSK144 signal is constant, before band limiting by filters in the transmitter.

Waveform Spectrum and Envelope

Figure 2 shows the average audio spectrum of an MSK144 signal as generated by *WSJT-X*. The carrier frequency $f_c = 1500$ Hz has been chosen to center the main spectral lobe in the available bandwidth of a typical SSB transceiver. The generated audio waveform has constant amplitude; however, band limiting by the transmitter's audio and RF filters will remove all spectral components above 3 kHz, so only the main lobe will be transmitted and the waveform will no longer have constant envelope. Table 1 shows some examples of the amount of envelope variation caused by different amounts of filtering. Figure 3 shows the measured spectrum of a received MSK144 signal at the receiver's audio output, as well as the spectrum of receiver background noise with no signal present.

Linear amplification is necessary to reproduce faithfully the envelope variations introduced when the MSK waveform is filtered. Such an amplifier will maintain the sidelobe-free spectrum produced by the transmitter filter. On the other hand, if the signal is hard-limited and then amplified by a nonlinear amplifier, spectral sidelobes will reappear, but at lower levels than were present before filtering.[5] In general, we expect that the MSK144 waveform will tolerate nonlinear amplification without generating excessive amounts of splatter; however anyone contemplating use of a nonlinear amplifier should conduct tests to verify that the amplifier does not cause excessive spectral broadening.

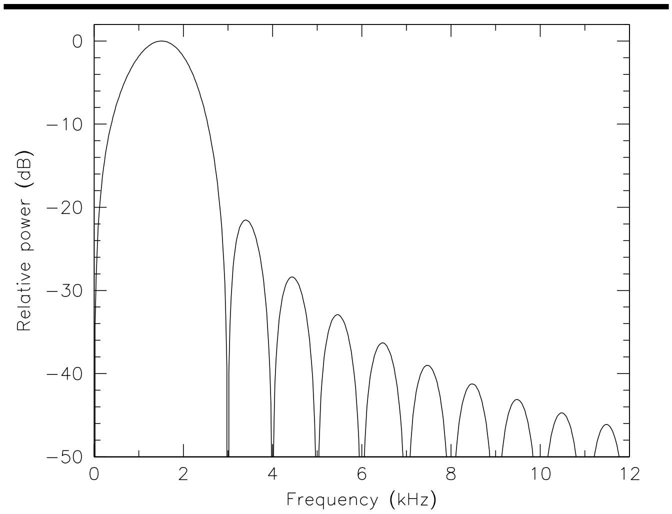

Figure 2 — Average spectrum of MSK144 audio signals generated by *WSJT-X* using 1.5 kHz audio carrier frequency. Transmitter audio and RF filters will limit the bandwidth of the transmitted signal to, typically, 300-2700 Hz, which includes most of the main lobe of this spectrum but no sidelobes.

Frame Structure and Channel Code

As in all other *WSJT-X* modes with FEC, MSK144 user messages are compressed into exactly 72 bits. Transmissions consist of a sequence of identical frames that carry these bits along with synchronizing and error-correcting information. Each frame includes a 72-bit user message, an 8-bit *cyclic redundancy check* (CRC) computed from the message, and 48 bits of error-correcting redundancy. The resulting 72 + 8 + 48 = 128-bit *codeword* is combined with two 8-bit sync words to form a 144-bit message frame. The frames are constructed as {S8, D48, S8, D80}, where S8 represents an 8-bit sync word and D48, D80 represent the first 48 and last 80 bits of the 128-bit codeword. The 8-bit CRC is used by the decoder to detect and eliminate most false decodes. At 2000 baud, the frame duration is 144/2000 = 0.072 s.

The 80-bit combination of message and CRC is mapped to a 128-bit codeword using a binary (128, 80) *Low Density Parity Check* (LDPC) code designed specifically for MSK144. We chose an LDPC code because these codes provide state-of-the-art performance and can be designed with virtually any desired number of data bits and parity bits. Moreover, they can be decoded with low computational cost compared to other code types used in *WSJT-X* — specifically, the long constraint-length convolutional codes used in JT4, JT9, and WSPR and the Reed-Solomon code used in JT65. As a consequence

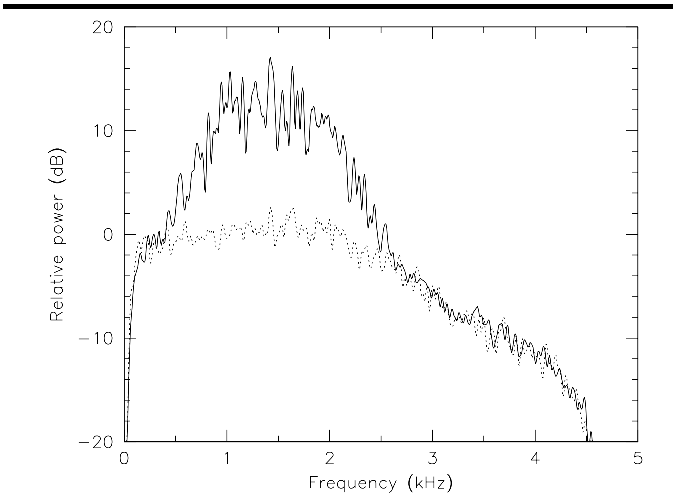

Figure 3 — *Solid curve:* received spectrum of the message "K9AN AA2UK R-05" transmitted by AA2UK and received by K9AN. *Dotted curve:* spectrum of background noise as shaped by the frequency response of K9AN's receiver.

Table 1

Representative examples of envelope variation obtained by filtering a simulated MSK144 frame. Envelope variation increases significantly as transmitter bandwidth narrows.

	Average power	*Peak envelope power*	*Peak-to-average power ratio*	*Max-to-Min power ratio*
No filtering	1.0	1.0	1.0	1.00
0-3 kHz	0.996	1.27	1.28	1.91
0.3-2.7 kHz	0.988	1.32	1.33	2.29
0.5-2.5 kHz	0.959	1.50	1.57	3.31

we can use many decoding attempts on each chunk of data, with each attempt concentrating on a different subset or weighting of the data. This procedure leads to a significantly higher probability for decoding weak or noisy signals.

The selected (128, 80) LDPC code is defined by a 48 × 128 *parity-check matrix* in which all elements are 0 or 1. The matrix has exactly three ones in each column and eight in each row. (Thus, only 3 × 128 = 8 × 48 = 384 of the 6144 entries are equal to 1; it's this low density of nonzero elements in the matrix that gives the LDPC code its name.) Each of the 48 rows of the parity check matrix defines a parity check equation. The eight 1s in each row determine which of the 128 codeword bits are included in that parity check. Each parity check is carried out by summing, modulo 2, the indicated codeword bits. All 48 of these sums will be zero for a valid, error-free codeword.

Starting with the parity-check matrix we derive a 48 × 80 *generator matrix* that will determine 48 parity bits for any 80-bit message word. The 1s in a particular row of the generator matrix determine which of the 80 message bits to sum, modulo 2, to produce a parity bit. Additional details of the way we have implemented these processes, including concise definitions of the two matrices, can be found in the open source code[6] for *WSJT-X*.

Code Performance

Figure 4 summarizes performance of the MSK144 protocol when used with the soft-decision decoder currently implemented in *WSJT-X*. As shown by the curve labeled P_c, single received frames with $SNR > 0$ dB are nearly always decoded correctly. (Here and elsewhere in this paper, signal-to-noise ratios are measured in a 2500 Hz standard reference bandwidth.) At $SNR = -1.5$ dB about 40% of received frames are correctly decoded, and about 0.1% of received frames will yield an incorrect codeword. Most of the incorrect codewords will be rejected because the falsely decoded message will not pass the CRC test. For *SNR*s near the 50% decoding threshold about 1 in 200 such incorrect codewords — about 5 per one-million decoding attempts — will accidentally have the correct CRC and will be displayed as *undetected false decodes*. The measured probability of undetected false decodes is plotted as a function of *SNR* as P_i, scaled up by a factor of 10^5 to make it visible on the plot. The false decode rate falls to negligible levels when $SNR > 0$ dB.

Figure 5 shows the fraction of noisy received codewords that will be decoded as a function of the number of hard errors in the codeword. Redundancy provided by the parity bits allows decoding of most synchronized frame-length bit sequences with fewer than 10 hard errors, and a small fraction of those with as many as 15 errors. We note that without the error-correcting code, even one hard error in the 72-bit packed message would reduce its uncompressed content to garbage.

A number of significant design choices have been built into the code/decoder combination. One such parameter is the number of iterations the decoder is allowed to try before it gives up. More iterations take more time, but (up to a point) will produce more decodes. However, the probability of false decodes increases dramatically if the maximum allowed number of iterations becomes too large. Another choice involves the detailed design of the code

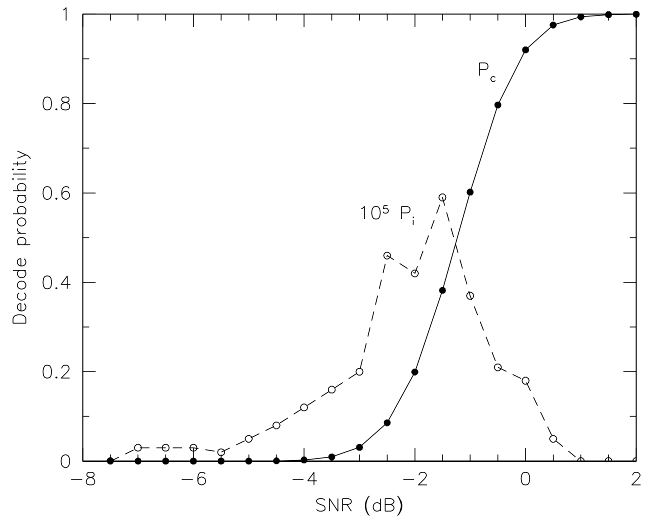

Figure 4 — Probability of a correct decode P_c and incorrect decode P_i as a function of *SNR* for standard MSK144 messages. These curves were generated by numerical simulation, based on 10^7 simulated noisy received frames. The results represent ideal performance assuming perfect frequency and time synchronization. Coherent averaging of *N* messages will slide both curves to the left by the amount 10 $\log_{10} N$.

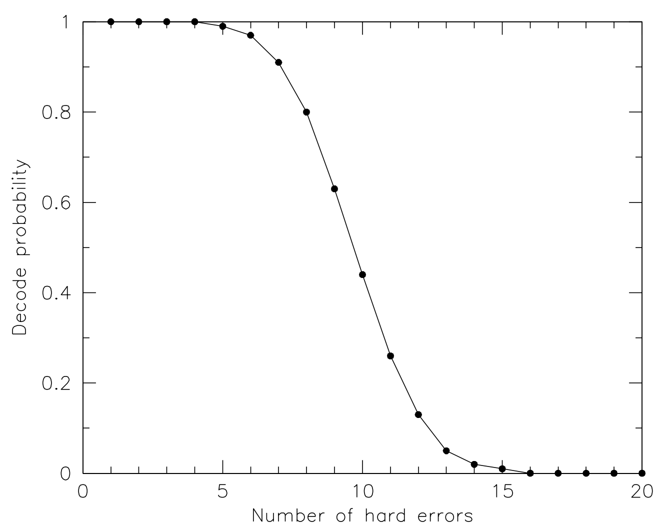

Figure 5 — Fraction of correct decodes as a function of the number of hard errors in a received codeword.

itself. Increasing the density of the parity-check matrix yields a code that requires more iterations to decode or, equivalently, produces fewer decodes for a given number of iterations. On the other hand, a more dense code that produces half as many decodes may give one fifth as many false decodes. We created a number of codes with different densities and explored the performance of each one for different iteration limits. Ultimately, we chose parameters that yield good P_c and P_i performance with the smallest number of decoder iterations. We believe the chosen code is close to optimum for the purpose at hand.

Optional Short-Message Format

On a given meteor-scatter path the duration of a ping is proportional to the inverse square of operating frequency. Pings at 144 MHz are therefore about 1/8 as long as those at 50 MHz. Most of a frame must be received in order to decode its message, so pings shorter than about 70 ms, common at 144 MHz and higher bands, are too short to convey a decodable standard MSK144 frame. To utilize even shorter pings, the protocol includes optional short messages that can be used to send signal reports and other necessary QSO information after call signs have been exchanged. Short frames are 20 ms long and consist of 40 bits: an 8-bit sync word, 4 bits to convey message information, 12 bits representing a hash of the string consisting of the DX call sign followed by the home call sign, and 16 parity bits for FEC. There are just 9 supported messages, namely R-03, R+00, R+03, R+06, R+10, R+13, R+16, RRR, and 73. The 12-bit hash serves two purposes: it gives the receiving operator high confidence that a decoded frame was indeed intended for him, and it is used to reject most false decodes.

We designed a binary (32,16) LDPC code for the MSK144 short-message frames. The 16×32 parity-check matrix has exactly three 1s in each column and 5, 6, or 7 in each row. Performance measurements for this code (including verification of the hash test) are plotted in Figure 6. The decoding threshold is almost the same as for the long code, but the peak probability of false decodes is about 30 times larger — a consequence of the short code's smaller block length.

Implementation in *WSJT-X*

MSK144 is one of seven distinct operating modes in program *WSJT-X*. An overview of the design purposes and operating characteristics of each mode has been published in the *QST* article of Note 4, and many more details can be found in the *WSJT-X User Guide*.[7] We limit the discussion here to some particular features of MSK144 as presently implemented in *WSJT-X*.

Decoder Details

With pings longer than about 100 ms we can coherently sum multiple frames to improve the signal-to-noise ratio. The current MSK144 decoder can average up to 7 frames, about half a second of data. Coherent averaging of N frames improves sensitivity by 10 log N dB, so sensitivity improves rapidly for longer pings. Coherent averages of $N = 2, 3, 4, 5,$ and 7 frames with constant signal level yield gains of 3, 4.8, 6, 7, and 8.5 dB, respectively. These amount to very worthwhile improvements, even when the real-world signal levels are not constant over the averaging interval.

Coherent demodulation requires proper alignment of channel-symbol boundaries, precise knowledge of a received signal's carrier frequency, and an estimate of carrier phase. Averaging over multiple frames increases the necessary frequency precision in proportion to total signal duration. To ensure that carrier phase does not vary significantly over the averaging interval, 7-frame averaging requires that frequency be known to better than 1 Hz. In effect, the decoding algorithm must search all possible frequency offsets in some tolerance window using a 1 Hz step size, at the same time searching over time offsets to establish symbol synchronization. For the longest frame averages, the decoder's execution time is dominated by this synchronization requirement.

WSJT-X implements a version of the *sum-product algorithm* [8] for soft-decision decoding of the noisy received symbols. This iterative decoding algorithm accepts a numerical reliability measure for each of the received symbols. Each iteration updates the symbol reliability based on the degree to which the parity check sums are satisfied. After every iteration, hard decisions are made about the value of each symbol based on the updated symbol reliabilities; if the result is a valid codeword, the algorithm terminates. If no codeword is found before completing a predetermined maximum number of iterations, the algorithm "times out" and reports a decoding failure.

The MSK144 decoder in *WSJT-X* Version 1.7 operates in near real-time by looking at small overlapping chunks of data and completing all decoding attempts before the next chunk arrives. Each chunk contains 7 message frames, equivalent to about 0.5 s of data. For each chunk the decoder first tries to synchronize and decode the best single message frames. If this fails, it tries combinations of 2-, 3-, 4-, and 5-frame coherent averages. Finally, it tries a coherent average of all 7 frames. Older and slower computers may not be able to keep up with the demands of the MSK144 decoder when using the "Deep" decoding setting on the *WSJT-X* user interface. Selecting "Normal" decoding will eliminate the longest and most time-consuming 7-frame average to save time. The "Fast" decoding setting eliminates both 5- and 7-frame averages. Omitting the longest averages reduces sensitivity somewhat, although the penalties are modest.

Phase Equalization

Most superheterodyne SSB transceivers use narrow filters optimized for good shape

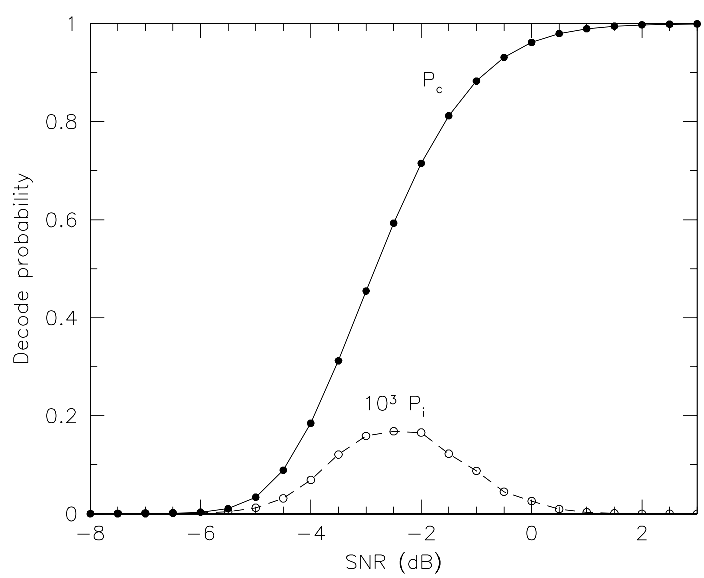

Figure 6 — Probability of a correct decode *P_c* and incorrect decode *P_i* as a function of *SNR* for the MSK144 short-message format. These curves were generated via numerical simulation, based on 10^7 simulated noisy received frames.

factor without regard to phase linearity. Group delay variation across the passband smears out MSK144 pulses, causing intersymbol interference. *WSJT-X* includes a phase equalization facility that can be used to correct any group delay variation contributed by the receiver. When a received frame has been successfully decoded, this tool generates an undistorted waveform whose Fourier transform can serve as a frequency-dependent phase reference to compare with the phase of the received frame's Fourier coefficients. Phase differences between the reference waveform and the received one will include distortions contributed by the originating station's transmit filter, the propagation channel, and filters in the receiver. If the received frame originates from a station known to transmit signals having little phase distortion (say, a station known to use a properly adjusted software-defined-transceiver) and if the received signal is relatively free from multipath distortion so that the channel phase is close to linear, the measured phase differences will be dominated by the local receiver's phase response.

The phase-response tool in *WSJT-X* fits a low-order polynomial to the measured phases. The saved polynomial coefficients can then be used to correct the phases in all received signals, effectively flattening the receiver's group-delay response. Careful use of this capability can improve the decoder sensitivity by significant amounts. As an example, Figure 7 shows the phase response of the TS-2000 receiver at K9AN, measured using a signal transmitted by the software-defined-transceiver at KØTPP. Phase errors as large as $\pi/2$ radians (90 degrees) are found near the passband edges, relative to mid-band values. The smooth curve in Figure 7 is a 4th-degree polynomial fit to the measured data. The improved decoder sensitivity can be judged from the *eye diagrams* of Figure 8, which contain overlaid plots of 72 received-symbol amplitudes constituting one frame of the signal from KØTPP. The upper part of the figure shows the diagram before phase correction; the lower part after applying the fitted phase equalization curve. Notice that the eyes are more "open" after equalization. Wider eye opening means fewer bit errors at low *SNR*, and a higher likelihood of successfully decoding a noisy received frame.

If the operator is careful to ensure that the applied phase correction accurately represents the receiver's response, then the phase equalization derived from one strong reference station will improve decoding of signals from most other stations. It should be noted that phase equalization is not likely to improve decoding performance for those who use SDRs with linear-phase receive filters.

Standard Operating Procedures

In North America the highest MSK144 activity levels are found on 6 meters. QSOs are carried out with alternating transmit/receive (T/R) sequences 15 s long; a hundred watts and a modest antenna up 20 feet is sufficient for making lots of meteor-scatter contacts. By informal convention the standard 6 m "calling frequency" is 50.260 MHz. As described in our earlier mentioned *QST* paper of Note 4, most QSOs start with someone calling CQ and proceed roughly as follows:

```
1. CQ K1JT FN20
2.      K1JT K9AN EN50
3. K9AN K1JT -01
4.      K1JT K9AN R+03
5. K9AN K1JT RRR
6.      K1JT K9AN 73
```

Each station continues sending a given message until receiving the next message from the QSO partner. The signal reports conveyed in messages number 3 and 4 are measured signal-to-noise ratios in dB. By longstanding tradition, especially for weak-signal work on VHF and higher bands, a minimal contact is considered complete and suitable for logging after both call signs, signal reports or some other previously unknown information, and acknowledgments have been exchanged. The final "73" message is a courtesy; in the above example it lets K1JT know that his final acknowledgment was received and the contact is complete. Many users like to exchange 13-character free-text "chit-chat" at this point.

As an example of on-the-air usage of MSK144, the *WSJT-X* screen shot in Figure 9 shows a sequence of messages received at K1JT after he called CQ on 50.260 MHz. In a transmission starting at 11:30:00 UTC,

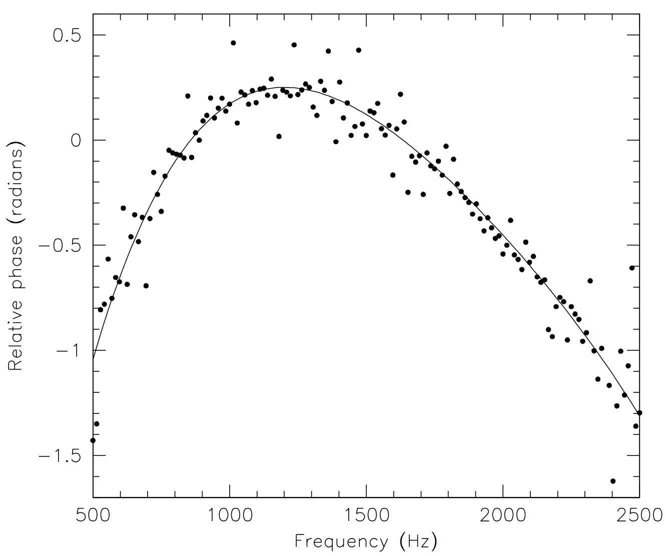

Figure 7 — *Filled circles:* measured phase differences between the complex spectra of a locally generated reference waveform and the average of several strong frames received from KØTPP. *Smooth curve:* 4th-order polynomial fit to the measured data.

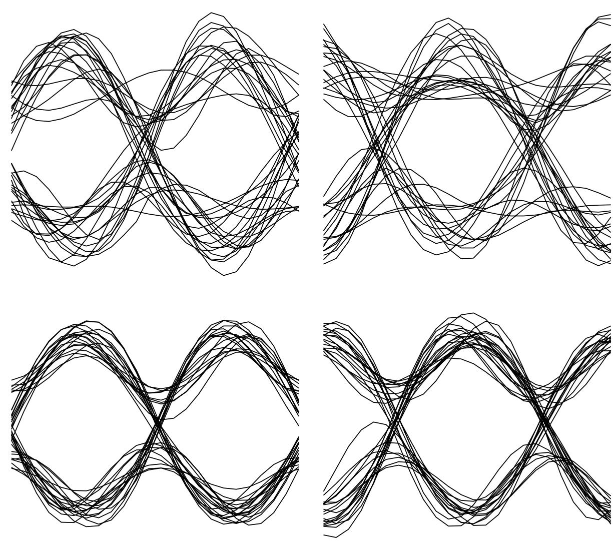

Figure 8 — Eye diagrams for the received in-phase (*left*) and quadrature (*right*) symbols for a signal from KØTPP received by K9AN. Upper curves are with no phase equalization; lower curves are after equalization using the polynomial fit shown in Figure 7.

W5ADD answered the CQ. Figure 10 is a snapshot of the *WSJT-X* horizontally scrolling spectrogram showing this ping (lower panel) and another one several sequences later that carried the message "K1JT W5ADD R-02" (upper panel). These two pings were of moderate strength, *SNR* = 5 and 4 dB, respectively, and the one in the top panel is about 70 ms wide; nevertheless these and even much weaker pings (see the "dB" column in Figure 9) are decoded without error. From Figure 9 you can see that when the QSO with W5ADD was complete N9BX and KA9CFD called as "tail-enders," and two more QSOs followed in quick succession.

UTC	dB	T	Freq		Message
113000	5	8.8	1565	&	K1JT W5ADD EM40
113230	4	11.4	1567	&	K1JT W5ADD R-02
113330	-1	1.6	1571	&	K1JT W5ADD 73
113530	5	6.3	1563	&	K1JT N9BX EM50
113600	-4	9.8	1570	&	K1JT KA9CFD EN40
113630	3	1.7	1560	&	K1JT N9BX EM50
113730	9	14.3	1558	&	K1JT N9BX R+02
113830	3	8.1	1559	&	K1JT N9BX 73
114030	2	14.0	1562	&	K1JT KA9CFD R+02
114530	14	13.4	1564	&	K1JT KA9CFD 73

Figure 9 — Messages received at K1JT in a sequence of three quick MSK144 QSOs on 6 meters.

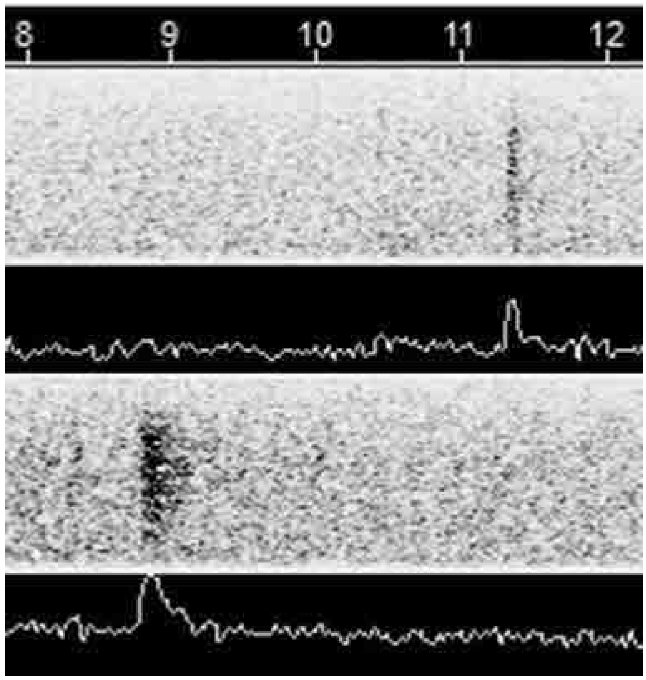

Figure 10 — Small portions of the *WSJT-X* real-time spectrogram showing pings received from W5ADD in sequences starting at UTC 11:30:00 (*lower*) and 11:32:30 (*upper*). The corresponding decoded messages are those in the first two lines of the screen shot in Figure 9.

Split Operation using "CQ nnn"

The sporadic nature of meteor pings makes it possible for many stations to share a frequency with little interference. Decoding several different stations in the same receiving sequence lets you see "who else is on," in addition to the station you may be working. However, when the frequency gets *too* busy it's a good idea to spread out. *WSJT-X* provides a mechanism for doing this while preserving the important advantage of having a known "meeting place" for initiating contacts. CQ messages may include three digits between the CQ and call sign. For example, K9AN might send "CQ 290 K9AN EN50" on 50.260 MHz to indicate that he will listen for replies on 50.290 MHz, and continue the QSO there. Note that offset CQs are not the same as typical "split" operation on HF bands. When operating split, each operator transmits on one frequency and listens on another. MSK144 QSOs using "CQ nnn" are used to move a contact off the calling frequency to a single offset frequency where both stations will transmit and receive. *WSJT-X* has facilities that allow it to recognize "CQ nnn" calls and reset the transceiver's dial frequency automatically, as required for both stations.

Contest Mode

North American VHF contests use Maidenhead grid locators as multipliers and required exchange information. MSK144 offers an optional *contest mode* in which grids are exchanged and acknowledged instead of signal reports. The standard message sequence then becomes

```
1. CQ K1JT FN20
2.      K1JT K9AN EN50
3. K9AN K1JT R FN20
4.      K1JT K9AN RRR
5. CQ K1JT FN20
```

The acknowledgment "R" in message number 3 is conveyed by using the fact that propagation modes suitable for MSK144 are generally effective only out to distances of order 1300 miles. To convey the message

UTC	dB	T	Freq		Message
120300	1	9.7	1497	&	CQ K9AN EN50
120300	2	10.5	1499	&	CQ K9AN EN50
120400	-1	11.9	1497	&	K1JT K9AN +03
120430	3	0.6	1496	&	<K1JT K9AN> RRR
120500	-2	9.4	1495	&	<K1JT K9AN> 73

Figure 11 — Messages received at K1JT in a QSO with K9AN using short-format messages.

We Design And Manufacture To Meet Your Requirements
*Protoype or Production Quantities

800-522-2253

This Number May Not Save Your Life...

But it could make it a lot easier! Especially when it comes to ordering non-standard connectors.

RF/MICROWAVE CONNECTORS, CABLES AND ASSEMBLIES

- Specials our specialty. Virtually any SMA, N, TNC, HN, LC, RP, BNC, SMB, or SMC delivered in 2-4 weeks.
- Cross reference library to all major manufacturers.
- Experts in supplying "hard to get" RF connectors.
- Our adapters can satisfy virtually any combination of requirements between series.
- Extensive inventory of passive RF/Microwave components including attenuators, terminations and dividers.
- No minimum order.

NEMAL
Cable & Connectors
for the Electronics Industry

NEMAL ELECTRONICS INTERNATIONAL, INC.
12240 N.E. 14TH AVENUE
NORTH MIAMI, FL 33161
TEL: 305-899-0900 • FAX: 305-895-8178
E-MAIL: INFO@NEMAL.COM
BRASIL: (011) 5535-2368

URL: WWW.NEMAL.COM

fragment "R FN20", *WSJT-X* encodes the locator as that of the diametrically opposite spot on Earth. The receiving program recognizes such a locator as special — it would imply an implausible distance approaching half the circumference of the Earth — so the software does the reverse transformation to the original grid and inserts the implied "R " in the message displayed to the user.

Short Messages

As described above, MSK144 supports short-form messages that can be used after QSO partners have exchanged both call signs. Short messages consist of 4 bits encoding R+report, RRR, or 73, together with a 12-bit hash code based on the ordered pair of "to" and "from" call signs. When short messages have been activated on the *WSJT-X* user interface, messages 4 to 6 in the standard sequence are modified as follows:

```
1. CQ K1JT FN20
2.      K1JT K9AN EN50
3. K9AN K1JT -01
4.      <K1JT K9AN> R+03
5. <K9AN K1JT> RRR
6.      <K1JT K9AN> 73
```

Individual call signs are replaced by a 12-bit hash code in the transmitted frame, and the substitution is indicated onscreen by enclosing the call signs in < > angle brackets. When the receiving program decodes the already known (and therefore expected) hash code, it displays the known call signs in angle brackets. Figure 11 is a screen shot showing messages received by K1JT in a QSO with K9AN using short messages. The short-message feature is intended for use on 144 MHz and higher bands, where very short pings make them especially beneficial.

A third party monitoring short message transmissions will not necessarily know the call signs of the stations involved in the ongoing QSO. *WSJT-X* implements an "SWL" mode that lets a listener monitor short messages exchanged by two other stations. When SWL mode is turned on, the decoder remembers recently copied call signs and compares received hashes with a list of hashes calculated from all ordered pairs of call signs currently in the list. If the received hash is found in the list, the decoder prints the decode with the "guessed" call signs in < > angle brackets. Accepting received messages with any hash found on a list increases the probability of printing a false decode in proportion to square of the number of remembered call signs. To decrease the number of spurious decodes printed in SWL mode, the software only prints decodes after the associated hash has been received at least twice in a receive sequence.

Conclusion

MSK144 is a highly efficient protocol for conducting minimal QSOs via meteor scatter. Indeed, we believe the protocol's effective character transmission rate, occupied bandwidth, and sensitivity are close to optimum for the stated purpose, while remaining consistent with the capabilities of standard amateur SSB transceivers.

We thank Bill Somerville, G4WJS, for helpful comments on an earlier version of this manuscript.

Steve Franke, K9AN, holds an Amateur Extra class license. He was first licensed in 1971 and has previously held call signs WN9IIQ and WB9IIQ. An early and abiding fascination with radio science led to his current position as Professor of Electrical and Computer Engineering at the University of Illinois in Urbana-Champaign. Steve is a member of ARRL and a Fellow of the IEEE.

Joe Taylor was first licensed as KN2ITP in 1954, and has since held call signs K2ITP, WA1LXQ, W1HFV, VK2BJX and K1JT. He was Professor of Astronomy at the University of Massachusetts from 1969 to 1981 and since then Professor of Physics at Princeton University, serving there also as Dean of the Faculty for six years. He was awarded the Nobel Prize in Physics in 1993 for discovery of the first orbiting pulsar, leading to observations that established the existence of gravitational waves. After retirement he has been busy developing and enhancing digital protocols for weak-signal communication by Amateur Radio, including JT65 and WSPR. He chases DX from 160 meters through the microwave bands.

Notes

[1]O. G. Villard, W6QYT, and A. M. Peterson, W6POH, "Meteor Scatter — A Newly Discovered Means for Extended-Range Communication in the 15- and 20-Meter Bands," *QST*, Apr. 1953, pp 11-15, 124, 126.

[2]Shelby Ennis, W8WN, "Utilizing the Constant Bombardment of Cosmic Debris for Routine Communication," *QST*, Nov. 2000, pp 28-32.

[3]Joe Taylor, K1JT, "*WSJT*: New Software for VHF Meteor-Scatter Communication," *QST*, Dec. 2001, pp 36-41.

[4]Joe Taylor, K1JT, Steve Franke, K9AN, and Bill Somerville, G4WJS, "Work the World with *WSJT-X*," (Scheduled) *QST*, Oct., and Nov. 2017.

[5]T. Aulin and C. Sundberg, *International J. Satellite Communications*, vol 2, p 219, 1984.

[6]**sourceforge.net/projects/wsjt**.

[7]**www.physics.princeton.edu/pulsar/K1JT/wsjtx-doc/wsjtx-main-1.7.1-devel.html**.

[8]Shu Lin and Daniel J. Costello, *Error Control Coding*, Pearson Prentice Hall, 2004.

DX ENGINEERING®

Showroom Staffing Hours:
9 am to 5 pm ET, Monday-Saturday

Ordering (via phone):
8:30 am to midnight ET, Monday-Friday
8:30 am to 5 pm ET, Weekends

Phone or e-mail Tech Support: 330-572-3200
8:30 am to 7 pm ET, Monday-Friday
9:00 am to 5 pm ET, Saturday
All Times Eastern I Country Code: +1
DXEngineering@DXEngineering.com

800-777-0703 | DXEngineering.com

Improve Your Station's Performance with DX Engineering!

SB™

SOTABeams' WSPRlite Antenna Performance Analysis System—Available Exclusively in North America from DX Engineering
WSPRlite is a specialized WSPR test beacon that transmits to a worldwide network of receiving stations. It works with SOTAbeams' proprietary software to display a transmit signal's geographical range as well as received power on an easy-to-read propagation map. WSPRlite is entirely self contained and covers the 20 & 30 meter bands. An optional 160/80/40 meter kit is available too.

DX ENGINEERING®

NCC-2 Receive Antenna Variable Phasing System
The NCC-2 now combines the NCC-1 Phase Controller and our RTR-1A Receive Antenna Interface technologies into one box. It also has enhanced balance functionality, expanding its ability to phase between two different types of antennas. This is a handy feature if you've got space constraints on your property. We've also made it easier (and more economical) to expand the NCC-2's versatility by providing internal slots for modules like the new plug-in versions of our Receiver Guard 5000HD and RPA-2 preamplifier.

plasticase NANUK™ PROFESSIONAL PROTECTIVE CASES RigExpert®

Analyzer and NANUK Case Combos
In the field, an antenna analyzer is especially at risk for weather and shock damage. We've paired select RigExpert Antenna Analyzers with perfectly sized NANUK equipment cases. Each case is filled with cubed, sectioned foam for custom configuration. Find detailed information on each analyzer and case at DXEngineering.com.

DX ENGINEERING®

Automatic Band-Pass Filter
Select from one of six band-pass filters with the simple push of a front-panel button. DX Engineering's Automatic Band-Pass Filter comes preloaded with filters for the 160, 80, 40, 20, 15 and 10 meter bands. With over 40 dB of stop-band rejection, each filter effectively removes unwanted and interfering noise and signals from all but the single band you have selected.

KENWOOD ICOM YAESU ALINCO

Request Your New Catalog Today!

Robert J. Zavrel, W7SX

PO Box 28756, Spokane, WA 99228; **w7sx@arrl.net**

Summing Electromagnetic Fields and Power From and To Antennas

W7SX explains field-strength and power combining in various configurations of dipoles and dipole arrays.

A common source of confusion when considering radiating and receiving radio waves is the relationship between power, *P*, and the fields associated with the wave. Here we will deal with only the electric field, **E**, behavior. I will attempt to explain how waves reinforce and cancel, and offer several examples for clarification.

The characteristics of electromagnetic waves are precisely defined by a set of linear equations known as Maxwell's Equations. In physics, the principle of superposition applies to linear equations, and therefore also applies to problems involving electromagnetic fields. The magnetic, **B**, and electric, **E**, fields, which comprise an electromagnetic wave are mathematically defined as vectors. When superposition applies, simple vector summation and subtraction is valid for problems involving wave reinforcement and cancellation. Examples of wave reinforcement and cancellation are familiar to amateurs who study the formation of antenna patterns from multi-element arrays as well as ground reflections. The examples presented here will include both of these situations.

From the above discussion we can now state the fundamental mechanism for the summing and canceling of radio waves: *at a given point in space, the total value of the E-field is the sum of all E-fields from all sources at that instant in time.* For our purposes, we may add the caveat that the sum of these *E*-fields come from the same source, that is, from the same transmitter. But in some examples, the transmit power will feed more than one antenna element.

Confusion arises from the fact that if you sum two identical **E** fields, the **E** value doubles, but that means the *power flux* quadruples! So the typical question is: how can I quadruple the power (6 dB) at a distant point by using a two-element driven broadside array if it will only have a gain of 3 dB over a single element? 3 dB gain is *doubling the power!*

First, we define the power density P_d that constitutes a radio wave in units of W/m^2 as,

$$P_d = \frac{E^2}{Z_0} \qquad (1)$$

that carries the units (V/m)^2 divided by Z_0, the intrinsic impedance of free space. Z_0 is equal to about 377 Ω. *E* is in V/m and is referred to as the *field strength*.

(1) The simple case of a half-wave transmit dipole and an identical half-wave dipole receive antenna

Figure 1 introduces the terms used in all examples and provides a reference for the subject power and gain terms. All examples are based on 100 W output from the transmitter. The distance between the transmit and receive antennas is *d* such that 100 W multiplied by the gain of the dipole will result in an *E* field of 1 V/m at our test receiver locations. We will also normalize the wavelength λ to 1 m (300 MHz) to simplify the equations. Since we are interested only in the discussion of how power and fields are related in these examples, we need only the above terms. Some additional terms will be derived from the above in later examples.

Figure 1 shows a very basic radio link.

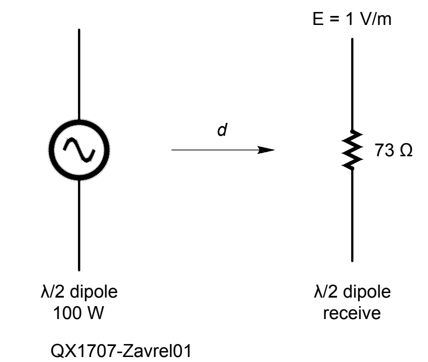

Figure 1 — The simple case of a half-wave transmit dipole and an identical half-wave dipole receive antenna.

The power gain of the receive dipole is 1.64 (2.15 dBi). Therefore the power delivered to the load impedance (the receiver) is the power flux of the radio wave at the receiver location, Eq (1), multiplied by the effective aperture of the receive antenna. So,

$$\begin{aligned} P_{received} &= SA_e \\ &= \left(\frac{1\,\mathrm{V}^2}{377\,\Omega\mathrm{m}^2}\right)\left(\frac{1.64\lambda^2}{4\pi}\right) \qquad (2) \\ &= 346 \text{ microwatts} \end{aligned}$$

where the first parentheses is *S*, the power flux in watts per square meter and the second parentheses is A_e, the effective receiving aperture in square meters.

The effective aperture area A_e of a half-wave dipole is the power gain, 1.64, relative to an isotropic antenna multiplied by the

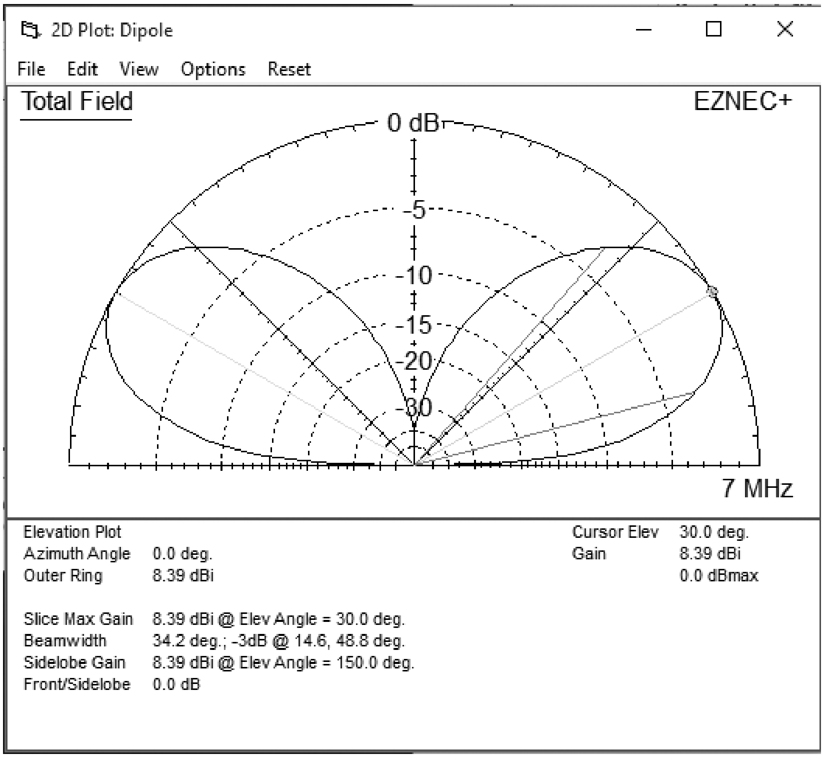

Figure 2 — *EZNEC* simulation of a dipole parallel to, and half wavelength above, a perfectly conducting ground.

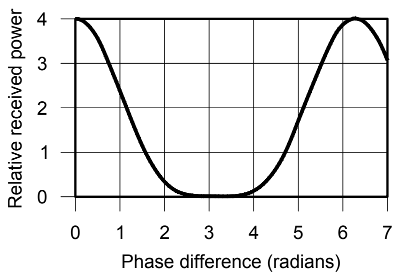

QX1707-Zavrel03

Figure 3 — This plot shows the effect of a perfectly reflected wave (ground reflection is a common example) upon an incident wave as the phase between the incident and reflected waves varies.

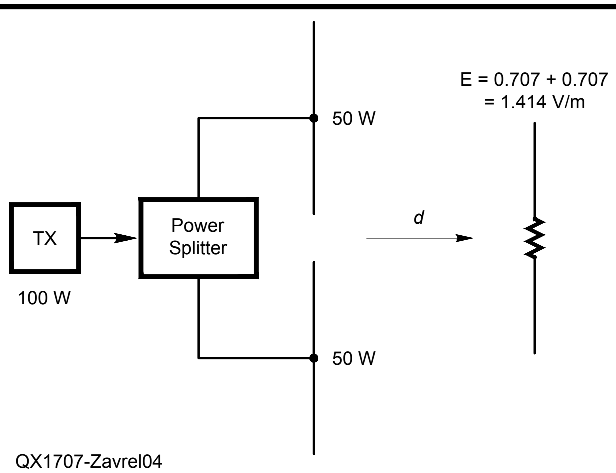

QX1707-Zavrel04

Figure 4 — Two half- wave dipoles configured as a two-element broadside transmitting array, with a single receiving dipole.

aperture area $\lambda^2/(4\pi)$, of an isotropic antenna. This example shows the basic mechanisms of the radio link. More detailed discussions appear in the Kraus[1] and Zavrel[2] references. With these terms defined we can now address some more complex examples.

(2) Power reinforcement at the elevation angle where the incident and ground-reflected waves perfectly combine

In this example we use an *EZNEC*[3] plot of the broadside gain of our half-wave dipole. Since the ground in this example is an infinite perfect conductor, the frequency does not matter, so 7 MHz will show identical results to 300 MHz. In this case, the power gain from the incident field will simply be the broadside gain of the dipole alone (2.15 dBi). However, the reflected field *doubles* the value of **E** in the far field thus *quadrupling* the equivalent isotropically radiated power (EIRP) at this critical angle (in this case 30 degrees elevation).

Figure 2 shows an *EZNEC* plot of a half-wave dipole at half-wavelength height above a perfectly conducting ground plane. The total E field in the far zone is,

$$E_{total} = E_{incident} + E_{reflected} \tag{3}$$

Since we have perfect reflection, the total field is $2E_{incident}$ Again since power is proportional to E^2 the added power of the reflected wave is a factor of 4, or 6 dB. Thus we would expect the total gain to be,

$$G_{total} = 2.15 \text{ dBi} + 6 \text{ dB} = 8.15 \text{ dBi} \tag{4}$$

We actually see 8.39 dBi in the *EZNEC* result. The small difference is due to the effects of a mutual impedance between the dipole and ground. In this case the dipole is a half wavelength above the ground.

This example shows why ground-reflected reinforcement can generate very impressive EIRP values at specific elevation angles. Over "real" ground the reflection coefficient becomes less than one, so the resulting gain is lower than this idealized case. The actual reflection coefficient is a function of the ground (soil) permittivity and conductivity, and therefore is a function of the frequency.

Figure 3 shows the effect of a perfectly reflected wave (ground reflection is a common example) upon an incident wave. The Y axis is the relative received power, where 1 is the normalized power value for the radiating antenna in free space. The X axis shows the phase difference between the reflected and the incident wave from 0 to 2π radians (0 to 360 degrees). Zero radians represents perfect reinforcement, while π

radians (180 degrees) represents perfect cancellation. The curve plots the function

$$Y = \left(1 + \cos X\right)^2 \qquad (5)$$

where 1 represents the normalized field strength of the incident wave and cos(X) represents the relative reflected field strength value as a function of the phase difference. The squaring provides the relative power value. The distance of the incident and reflected waves are assumed to be the same, and the reflection efficiency is perfect. Both these terms can be easily applied to the equation with a simple coefficient in front of the cosine term.

(3) Power receivedby a single dipole as transmitted by a two element array of half wave dipoles fed in phase with equal currents and one half wave spacing

Figure 4 shows two half-wave dipoles configured as a two-element broadside array. The gain of such an antenna has a theoretical maximum gain of about 3 dBd, or twice the gain of a single dipole.

With the single dipole transmit antenna in Figure 1, *all* 100 W is fed to the single antenna. This configuration was assumed to provide 1 V/m field strength at the distance *d*. However, in the two-element array, only 50 W is fed to each antenna. Therefore, the contribution of each antenna to the field at distance *d* will be 0.707 V/m. These fields will simply add, providing 1.414 V/m. Squaring the relative field strength, we get a relative power of two compared to the Figure 1 result. Therefore the array has a power gain of two over a single dipole antenna or 3 dBd. A common mistake is not remembering the necessary power splitter and thus 100 W is erroneously assumed in both antennas, and thus an array gain of 6 dBd is falsely calculated.

(4) Power received by a two-element broadside dipole array from a single dipole element transmit array

Figure 5 shows the reciprocal case of Figure 4. In this example, the same 1 V/m field strength is incident on both receive dipoles. However, when considering a receive antenna, it is necessary to realize that a single antenna is a power detector. The power it receives is calculated by Eq (2). The concept is quite simple. RF power density at a given point is defined as watts per square meter, or power per unit area. Therefore, the power received is directly proportion to the antenna aperture (or effective area).

To calculate the power received, we use Eq (2) to get 346 microwatts, and multiply by 2 since there are now two power detectors, and get 692 microwatts, representing 3 dBd gain, identical to Figure 4. When using two separate antennas the total power received is the sum of the powers received by each of the dipoles.

(5) Power received by a two-element co-linear receive antenna and a single dipole transmit antenna

Figure 6 shows a two-element collinear antenna that is actually a full-wave dipole. Indeed, the voltage induced in this antenna will be twice that of a half-wave dipole. Therefore, we might expect the two-element collinear to have 6 dB higher gain than a half-wave dipole. However, in this case, we need a few more terms to arrive at the actual approximate gain of 2 dBd.

A critical term defined here is the effective height, or more appropriately called effective length of an antenna. A passing wave, with identical polarization and with the antenna presenting its maximum aperture toward the wave front, will induce a voltage in the antenna proportional to

$$V = h_e E \qquad (7)$$

where V is the voltage induced in the antenna and h_e is the effective height of the antenna. Again, E is the field strength at the antenna. Effective height, or length, is

$$\frac{I_{ave}}{I_{\max}} \frac{l_{physical}}{\lambda}$$

or the average current along the antenna length divided by the maximum antenna current, then multiplied by the physical length of the antenna in wavelengths. A formal definition and calculation can be found in both listed references.

The current distribution along a dipole and a two-element collinear is nearly sinusoidal. In the case of a half-wave dipole,

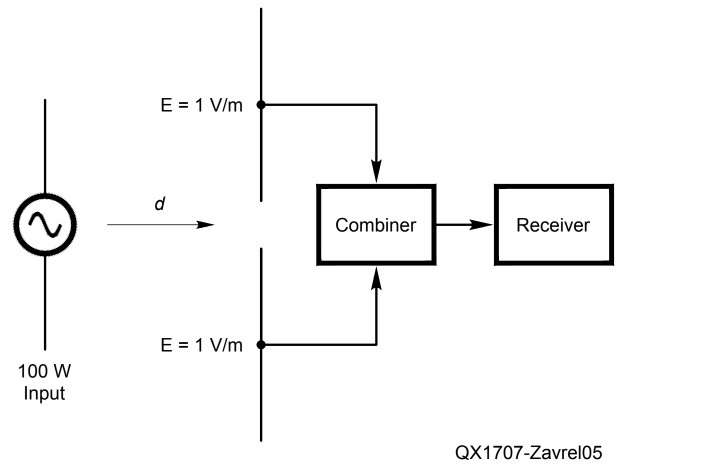

Figure 5 — Two half- wave dipoles configured as a two-element broadside receiving array, with a single transmitting dipole.

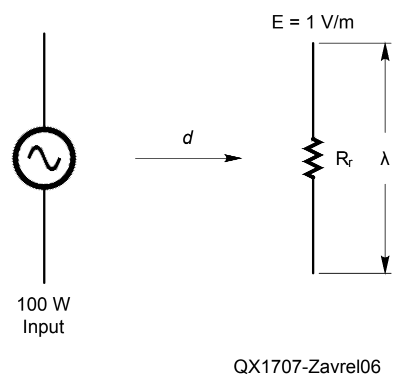

Figure 6 — A full-wave receive dipole antenna (two-element collinear) array

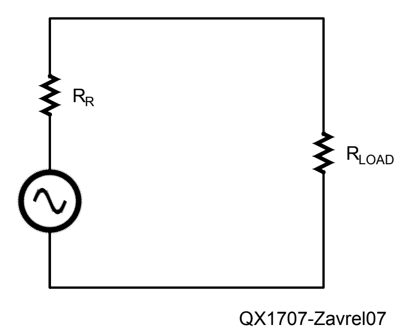

Figure 7 — An equivalent receive antenna R_R connected to a receiver load R_{LOAD}.

the current value forms a half-wave sinusoid distribution. The average value of a sine wave (normalized to a peak value of 1, and averaged over 0 to π) is 0.64. Therefore, the average value of the current on both antennas is 0.64 (assuming we normalize the maximum current to 1 A). However, h_e is 0.32 for the half-wave dipole and 0.64 for the full wave dipole since we must multiply the half-wave dipole average current by 0.5, and we have normalized the λ to 1 meter for simplicity.

Therefore, by Eq (7), the resulting voltage on the full-wave dipole will be twice the value of the half-wave dipole assuming the field strength is the same for both antennas. Again for simplicity we have normalized it to 1 V/m. This would imply that the power received by the full wave two-element collinear would be four times that of a half-wave dipole. This is not the case. The resolution of this involves some additional algebra.

Figure 7 shows an equivalent receive antenna connected — usually through a transmission line — to a load, which is usually a receiver. The antenna itself can be modeled as a voltage source along with a source impedance defined as the radiation resistance R_r. The receiver is R_{load}. When the two resistances are equal (a conjugate match), maximum power is transferred to the receiver, which is the usual desired condition. However, the power provided by the antenna to the receiver is a function of both the antenna voltage and these resistances. This is the resolution to the apparent paradox. We must know the radiation resistance of the antenna to calculate the power received, and thus also the antenna gain.

Radiation resistance can most easily be computed for this type of problem by the equation

$$R_r = \frac{h_e^2 Z_0}{4A_e} \tag{8}$$

from which we can also provide another definition for

$$A_e = \frac{h_e^2 Z_0}{4R_r} = \frac{G\lambda^2}{4\pi} \cdot \tag{9}$$

where R_r is the radiation resistance, h_e is the effective height, Z_0 is the intrinsic impedance of free space (377 Ω), G is the numeric gain of the antenna and A_e is the effective aperture of the antenna. The derivation of this equation can be found in references 1 and 2. We can find the gain, and thus the effective aperture of both the half-wave dipole and the one wavelength collinear dipole by using *EZNEC*. The dipole numeric gain is 1.64 and the collinear is 2.39, both referenced to the isotropic antenna gain of 1.

For a half-wave dipole this works out to about 73 Ω. By re-arranging terms from Eq (2), (7) and (9) we can write,

$$P_{received} = SA_e = \left(\frac{E^2}{Z_0}\right)\frac{h_e^2 Z_0}{4R_r} = \frac{V^2}{4R_r}$$
$$= 504 \text{ microwatts}$$

for the power received by the two-element collinear antenna. Notice that 504 microwatts is definitely not four times 346 microwatts from the dipole example in Figure 2. Rather it conforms nicely, as we would expect, to the gain ratio between the two antennas of about 2 dB.

To conclude, for a single antenna element that generates twice the voltage from a field strength due to twice it's effective length, the radiation resistance limits the power gain. Also, up to relatively long linear (straight wire) antennas, as the antenna length is made physically longer, both the effective length and the radiation resistance increase thus limiting the power gain. The term $V^2/(4R_r)$ explains the paradox. (10)

Bob Zavrel, W7SX, was first licensed in 1966. He is an ARRL Technical Advisor and Life Member. He is author of the ARRL publication "Antenna Physics: an Introduction" and has published over 60 articles in amateur and professional publications. He has Honor Roll status for DXCC mixed and CW, using only tree-supported wire antennas. Bob has a BS in Physics from the University of Oregon and is currently working for Trimble Navigation as a senior R&D engineer.

Notes

[1]John Kraus, *Antennas*, McGraw Hill, 1988.
[2]Robert J Zavrel Jr., *Antenna Physics: An Introduction*, ARRL, 2016. ARRL item no. 0499, available from your ARRL dealer, or from the ARRL Store, Telephone toll-free in the US 888-277-5289, or 860-594-0355, fax 860-594-0303; **www.arrl.org/shop/**; **pubsales@arrl.org**.
[3]Several versions of *EZNEC* antenna modeling software are available from developer Roy Lewallen, W7EL, at **www.eznec.com**.

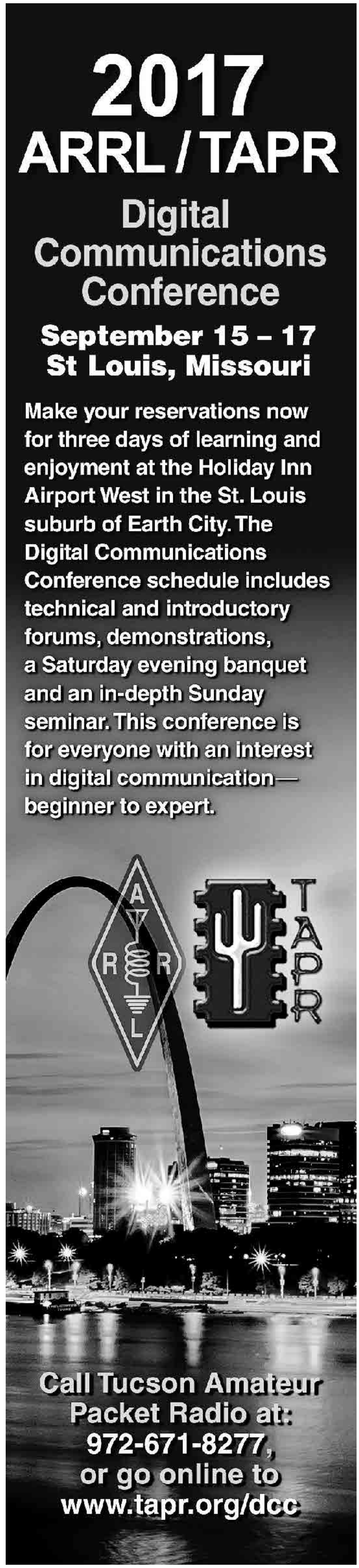

David Birnbaum, K2LYV

8515 Acorn Ridge Ct., Tampa, FL 33625: **dbirnbau@gmail.com**

Design of a Two-band Loaded Dipole Antenna

Calculate the LC trap values given the physical size of the antenna and two desired resonant frequencies.

I wanted to put up a dipole antenna in my attic but didn't have space for a full sized 40 meter antenna. I came across a *QST* article[1] by Luiz Lopes, CT1EOJ, on a method to calculate the values of loading coils to resonate a short antenna on a frequency lower than the natural resonant frequency. It dawned on me that if adding inductance would effectively lengthen an antenna then adding capacitance would effectively shorten it and that Lopes' method would work to find the capacitance as well.

A parallel *LC* circuit is inductively reactive below its resonant frequency, and a capacitively reactive above its resonant frequency. So if I replaced Lopes' loading coil with a parallel *LC* trap. I could find *L* and *C* values that would make the trap have just the right inductive reactance at one frequency to resonate an antenna at that frequency, and at the same time have the right capacitive reactance to make the antenna effectively shorter, and hence resonant, at some higher frequency. This article explains how to calculate the *LC* values given the physical size of the antenna and the two desired resonant frequencies.

Calculating the Reactances

We can compute the reactances needed at two specified frequencies using the method of Lopes. When we shorten the antenna we are removing a piece of the full size dipole and replacing the cut piece with an inductance. Figure 1 shows half of a dipole where the dashed part represents the piece removed to shorten the antenna. Only half of the dipole is shown since the locations of the loading elements will be symmetrically placed about the center. These calculations also apply to a loaded vertical antenna. The location of the piece and its length are both design choices. One sets the total length by some external constraint, then chooses the location of the cut to optimize some aspect of the antenna behavior. The needed inductive reactance value is given by the difference in reactance between points "A" and "B" in Figure 1. Note that if the antenna is too long it is the same as adding a negative gap to the normal dipole length.

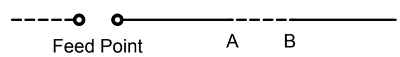

QX1709-Birnbaum01

Figure 1 — One side of a symmetrical loaded dipole shows the gap between A and B where length is removed and a trap is inserted.

Lopes models the antenna as a single-wire transmission line above ground. The reactance at any point along the transmission line is given by the transmission line equation, $Z = jZ_0 \tan(\beta)$, where Z_0 is the characteristic impedance of the transmission line and β is the distance in electrical degrees from the center of the antenna to some point on the antenna. β is between 0 and 90 degrees as we move out to a quarter wavelength along the dipole arm. For a single-wire transmission line above ground the characteristic impedance is,

$$Z_0 = 138 \log_{10}\left(\frac{4h}{d}\right)$$

where h is the height of the antenna above ground, and d is the diameter of the wire, both in the same dimensions.

Note that the placement of the trap is governed by the requirement that the inner length must be shorter than a quarter wavelength at the higher frequency. Given an antenna length and two frequencies at which we would like it to be resonant, we can use the method of Lopes to calculate the value of inductive reactance for the lower frequency and the value of the capacitive reactance at the higher frequency. These are the effective values, and we need a trap that would have these reactances at the two frequencies.

Parallel LC Network

The reactance of a parallel *LC* circuit is,

$$X(\omega) = \frac{-\omega L}{1 - \left(\frac{\omega}{\omega_0}\right)^2} \tag{1}$$

where ω_0 is the resonant frequency of the circuit. It is more convenient for our purposes to re-write this equation in terms of ω_0 and X_0 the magnitude of the reactance of either of the components at the resonant frequency. With some algebraic manipulation we get,

$$X(\omega) = \frac{-X_0}{\left(\frac{\omega_0}{\omega}\right) - \left(\frac{\omega}{\omega_0}\right)} \tag{2}$$

where $X(\omega)$ is the effective reactance of the trap at frequency ω.

We want the trap to have reactance X_1 at the lower frequency ω_1, and reactance X_2 at the higher frequency ω_2. From equation (2),

$$X_1 = \frac{-X_0}{\left(\frac{\omega_0}{\omega_1}\right) - \left(\frac{\omega_1}{\omega_0}\right)} \tag{3}$$

and

$$X_2 = \frac{-X_0}{\left(\frac{\omega_0}{\omega_2}\right) - \left(\frac{\omega_2}{\omega_0}\right)} \tag{4}$$

Divide equation (4) by (3) to eliminate X_0 to get an equation in terms of the reactance ratio at the two frequencies,

$$\frac{X_2}{X_1} = \frac{\frac{\omega_0^2}{\omega_1} - \omega_1}{\frac{\omega_0^2}{\omega_2} - \omega_2}$$

Since we know X_2 and X_1 we can solve this last equation for ω_0^2,

$$\omega_0^2 = \frac{\omega_1^2 \omega_2 - \frac{X_2}{X_1} \omega_2^2 \omega_1}{\omega_2 - \frac{X_2}{X_1} \omega_1}$$

We use this to solve for X_0,

$$X_0 = X_1 \left(\frac{\omega_1}{\omega_0} - \frac{\omega_0}{\omega_1}\right) = X_2 \left(\frac{\omega_2}{\omega_0} - \frac{\omega_0}{\omega_2}\right).$$

The *L* and *C* Values

Given the antenna length that one wants to use, and the desired two resonant frequencies, we can calculate ω_0^2 and X_0. From these we calculate the values of *L* and *C* that comprise the trap,

$$X_0 = \omega_0 L = \frac{1}{\omega_0 C} \text{ and } \omega_0^2 = \frac{1}{\sqrt{LC}}$$

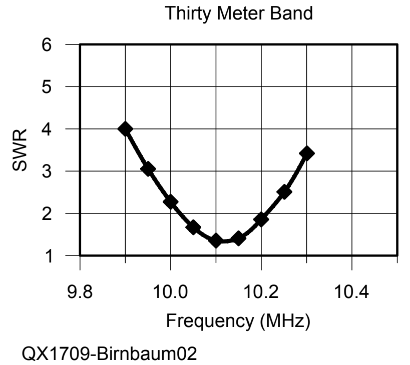

Figure 2 — SWR calculated using NEC for the 30 m band.

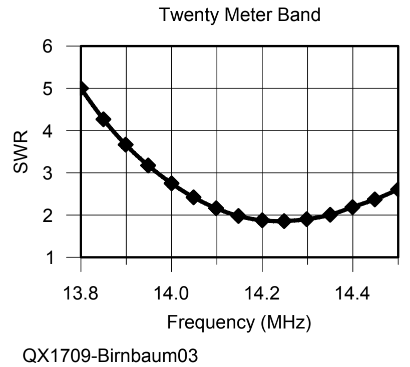

Figure 3 — SWR calculated using NEC for the 20 m band.

Finally,

$$L = \frac{X_0}{\omega_0} \text{ and } C = \frac{1}{\omega_0^2 L}.$$

The only remaining design parameter is where along the dipole arms to insert the trap. The Lopes design process gives the equations that calculate the *X* values needed for placing the trap at any location along the antenna arms subject to the constraint that the part of the antenna between the feed point and the trap must be less than a quarter wavelength at the higher frequency. In general we would like to keep as much of the center part of the full length dipole as possible since that is the part where the current, and hence the radiation, is highest. Also as we move the load towards the end of the antenna the values of the impedances needed increase rapidly.

Table 1
Design example for the 30 and 20 m bands

Antenna total length	40 feet
Antenna height	20 feet
Lower design frequency	10.1 MHz
Upper design frequency	14.05 MHz
Distance from center to trap	14 feet

Design Example

Here's a design example (see Table 1) for a 40 foot antenna that will work on the 30 and 20 meter bands. Using the above equations, the antenna has a characteristic impedance of 536 Ω. The required inductance is 2.94 µH and required capacitance is 52.7 pF.

Figures 2 and 3 shows SWR plots from a model of the above antenna using numerical electromagnetic code (NEC). To make the results more realistic, the optimal *L* and *C* values were changed to 3.0 µH and 53 pF.

Dave Birnbaum, K2LYV, holds an Amateur Extra class license. His previous calls were KN2LYV, W3GFC, WØOZX and W2IIV. Dave has a BEngr in Engineering Physics from Cornell University and MS and PhD in physics as well as an MBA from the University of Rochester. After teaching physics at the university level for several years, he transitioned to the General Railway Signal and then to Xerox Corp where he worked on digital imaging for color xerography and ink jet printing. Dave retired from Xerox as an Engineering Fellow in 2003. He holds 15 patents. In addition to ham radio, he plays the trombone in a few local concert bands. David is a member of the Tampa Amateur Radio Club and especially enjoys digital modes and CW. He has earned the WAS and DXCC awards.

Notes

[1]Luiz Lopes, CT1EOJ, "Designing a Shortened Antenna", *QST*, Oct, 2003, pp 28 – 32.

John E. R. White, VA7JW

344 Oxford Drive, Port Moody, BC V3H 1T2, Canada: **va7jw@shaw.ca**

Weatherproofing Experiment with PL-259 Connections

Water seepage into the PL-259 connector is common, and can significantly degrade the electrical properties of the connection.

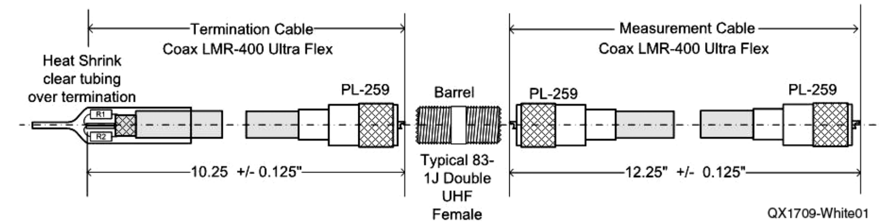

Figure 1 — Test cable construction.

The PL-259 is the dominant male coaxial cable connector used for indoor and outdoor coax cable connectivity. Outdoor service is far more demanding due to weather. The seepage of water into connections such as the PL-259 is common as they are not waterproof. This can significantly and quickly degrade the electrical properties of the connection. This experiment deals only with liquid water, not freezing issues, nor the effects of ultra-violet damage or temperature cycling issues. Pity the poor outdoor PL connector.

Most station transmission line systems have inserted components such as power and SWR meters, filters, switches, and of course PL-259 connectors. These items will present a characteristic impedance close to the $Z_0 = 50\ \Omega$ of the transmission line. However, even small variations from the transmission line Z_0 by such components will be seen as an impedance discontinuity to the forward wave propagating down the line. Discontinuities inherently result in a reflection of a portion of the forward power, which is reflected back to the source, and is lost.

Overall, the discontinuity is small and reflected power is minimal, so the PL-259 works well enough, provided the connection is *tight and dry*. "Water in the coax and connectors will manifest itself as loss, and will attenuate the transmitted incident power as well as reflect power due to mismatch. The SWR meter will report a lower SWR due to the attenuated reflected wave indicating better performance than is the actual case".

The SWR meter, commonly connected in-line, constantly advises us of the system SWR[1], indicating reflected power in part due to connector impedance discontinuities. Another way to measure impedance discontinuity is by Return Loss (RL). This is the ratio of forward power to reflected power expressed in decibels. Table 1 shows the relationship of SWR to RL in terms of percent reflected power.[2] In this experiment both SWR and RL are measured using the Array Solutions, AIM-4170 Antenna Analyzer over the frequency range 1 to 150 MHz

Weatherproofing Test

The question arises, "what techniques are most effective in protecting the connections?" A controlled experiment is needed to objectively measure the effectiveness of various weatherproofing techniques commonly employed to PL-259 connectors. This would require building a number of identical test cables, each being weatherproofed differently. Certain parameters would be measured under identical and consistently wet conditions. It is unclear how to do this outside in the weather, under widely varying ranges of temperature and moisture. Therefore, an indoor controlled environment, bench test, is needed to make valid comparisons.

This led to the construction of 8 identical test cables, using LMR-400-UF (Ultraflex) coax, each with a unique weatherproofing applied over a central PL-259 connection. Each of the 8 test cables(Figure 1) consists of

Table 1.
SWR, Return Loss, and Reflected Power.

SWR	1.1:1	1.2:1	1.3:1	1.4:1	1.5:1	2:1	3:1	4:1	5:1	10:1
RL, dB	26	21	18	16	14	9.5	6	4.4	3.5	1.7
Reflected Power, %	0.23	0.8	1.7	2.8	4	11	25	36	44	67

2 sub-cables. One sub-cable is terminated at one end with a metal film resistor trimmed to 50 Ω, within 0.1 Ω, and a PL-259 is connected to the other end. This is the *termination cable*. The second sub-cable cable is terminated at both ends with PL-259 connectors. This is the *measurement cable*. The two cables are joined with a female–female SO-239 style barrel, and weatherproofing is applied over the connection. The technique for assembling the PL-259 onto the coax cable is shown in the Appendix.

How to Test for Water

A continuous immersion process was used to accelerate the ingress of water and the rate of degradation of the connections. Measurements would be made in comfort over a few weeks at room temperature. A plastic tub was modified to hold cable joints under water keeping the connections continuously wet and the ends dry (Figure 2).

Weatherproofing Techniques

Five different commonly available waterproofing materials are listed.[3, 4, 5, 6] The eight cables were dressed using either singly, or combined materials according to Table 2. Two of the 8 cable preparations are shown here as examples. Figures 3A and 3B show Cable #1, an untreated connection with no waterproofing applied. Figure 4A and 4B, Cable #4, show the wrapping of the various tape layers. Each tape is overlapped 50%.

Table 2.
List of cables and water proofing techniques.

Cable 1	No weatherproofing applied.
Cable 2	Black Electrical Tape. Scotch® Super 88, a durable tape for the outdoor environment
Cable 3	Black Electrical Tape + a stretchable rubber, self-vulcanizing “ Fusion” tape
Cable 4	Black Electrical Tape + Fusion tape + Black Electrical Tape
Cable 5	STUF® a Dielectric Grease which fills voids and displaces water in a connection
Cable 6	STUF® + Black Electrical Tape
Cable 7	Black Electrical Tape + Coax Seal®, a hand-moldable, tacky, black plastic mastic
Cable 8	Generic Heat Shrink tubing with internal “Glue” that seals the connection

Figure 2 — The water bath with seven cables immersed, and one dry reference cable.

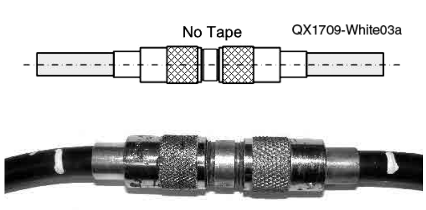

Figure 3 — An untreated connection with no waterproofing applied, (A) drawing and (B) image.

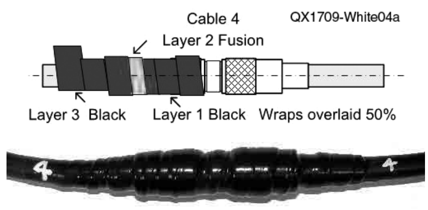

Figure 4 — The wrapping of the various tape layers, (A) drawing and (B) image. Each tape is overlapped 50%.

Test Plan

Each cable was characterized when dry, which established the “Base Line” against planned wet measurements. The dc resistance was measured using a Fluke 73 DVM. The dc termination resistance of all cables was trimmed to 50 Ω ±0.1 Ω. SWR and RL measured using the AIM 4170 Antenna Analyzer. All cables measured the same when dry. The cables were immersed and measured nominally at 1 day, 2 days, 6 days, 12 days and 22 days, to record change in dc resistance, SWR and RL. At the end of 22 days, each cable was stripped of its weather protection and examined for ingress of moisture.

Test Results

After 22 days wet, the change in performance is illustrated in Figure 5, the SWR and RL sweeps of all 8 cables. Half the cables exhibited significant degradation over the 22 wet days. All tapes were removed and all PL-259 connectors and barrels were inspected for water ingress. Deficiencies were noted, particularly with Cables #3, #4 and #6. Cable #1 was not expected to perform at all well, and it didn’t.

Erratic dc resistances were noted in some measurements with variations of greater than a few ohms to open-circuit under agitation of the joint. Some tapes lost adhesion and developed loose ends, and were starting to unravel. When a loose connection was noted the connector was not tight to the barrel. Water was observed under all the tapes.

The suspect cables (#3,# 4, and #6) were rebuilt with greater care and attention in the application of the weather proofing tapes, and those with STUF® were re-constructed ensuring that the connector to barrel mechanical connection was tightened to squeeze out surplus grease. The PL-259 shells were gently tightened with slip jaw pliers in all cases. Cable #2 performed beyond expectation. It was rebuilt to confirm the performance. The reworked cables were retested using the same techniques under the same 22 day regimen.

Re-Worked Test Results and Findings

The second batch of tests were much improved as seen in Figure 6. The graph shows the change in SWR and RL using day 0, dry as reference, to day 22, wet. Cable #1 was not expected to improve and did not. Cable #4 showed little improvement.

After the 22 day sweeps were completed, the weatherproofing materials were carefully removed and inspected as described earlier. The biggest surprise continued to be the ingress of water under *all* tapes. When removing the tapes, a totally unexpected leakage path was revealed as seen in Figure 7A and 7B. The over-lapping of tape as it is wound on the cable, appears to create an unavoidable, continuous, and miniscule void where the overlap steps down off the tape, on to the surface of the cable. This generates a spiral leakage path for moisture to wick along the cable surface up to the PL-259 connector. This wet path was observed when removing the tapes.

Given time, water variously accumulated on the PL-259 and barrel and shell. Once water appears on or around the PL-259 connector, it will likely enter the connection as illustrated in Figure 8. The most significant water ingress point is indicated by the upper arrowed line. A gap between the shell and the barrel of the PL-259 connector, varying by manufacturer, was variously measured from 0.01" to 0.05". This allows water to flow unimpeded all around the outside of, and along the barrel, onto the face of the connection where it can accumulate in the void between the connector faces. Moisture here would account for the significant effects seen on the SWR and RL graphs.

A lesser path exists as indicated by the lower arrowed line, where water wicks in between the outside of the coax jacket and the internal threads of the barrel. The connection is tight, but not waterproof. Water thus flows to the interior of the barrel and

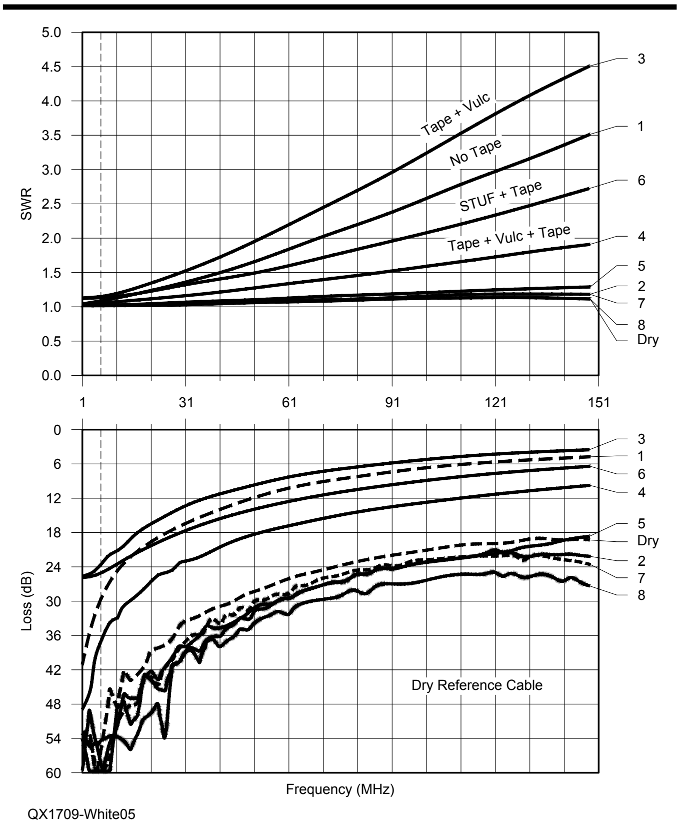

Figure 5 — First construction test results.

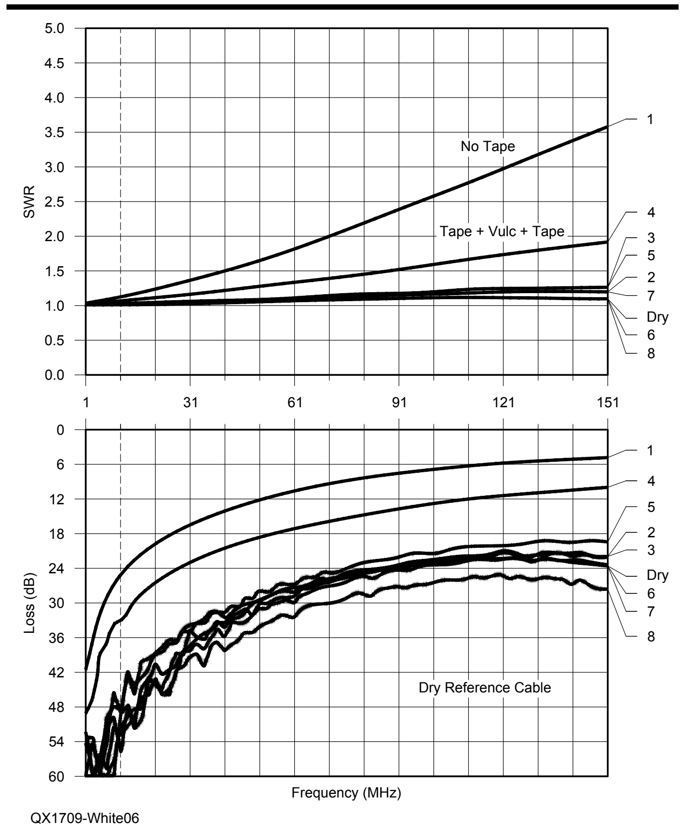

Figure 6 — Second construction test results.

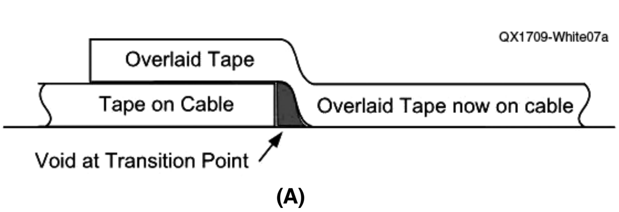

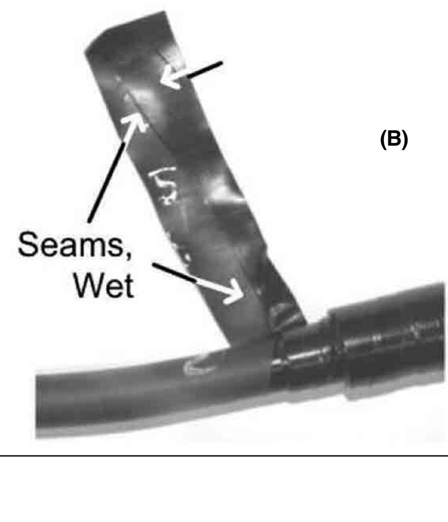

Figure 7 — Overlapping tape water channel follows the void (A), and can be seen (B) as a wet seam.

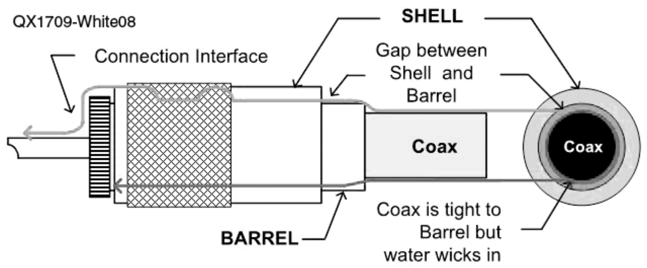

Figure 8 — PL-259 water ingress paths.

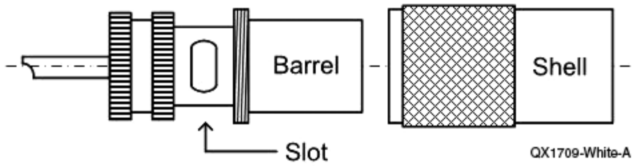

Figure A — PL-259 connector showing the shell, barrel and slot.

enters the chamber at the inside end of the barrel where the coax end has been exposed for soldering. This opens the possibly of water wicking into the coax itself. SWR and RL would further degrade.

The Bottom Line

Over the HF range, all cables came within a 2:1 SWR when assembly techniques were carefully applied. For VHF, degradation becomes more evident and greater attention to weatherproofing is advised. The effectiveness of various materials and methods is as follows.

Keeps Water Out

Heat shrink tubing or Coax Seal® will preserve the integrity of the connection. A heat gun (not flame) is required to perform the heat shrinking operation.

Probably Keeps Water Out

A very effective approach is to apply STUF® to the barrel face as well as the PL-259 face and the threads of the barrel and shell, then tighten. Wrap a layer of black electrical tape over the joint. Then use Coax Seal® to seal the ends of the black tape against leakage and prevent unraveling. This construction was later tested on its own for 21 days immersed. Performance did not change from day 0, dry. Still, moisture was detected under the tape. STUF® saved the day by filling the connection interfaces, displacing water, as none was seen.

Might Not Keep Water Out.

Tapes alone leak, as were seen by the wicking of moisture into the connection. Layering of tapes does not improve matters much as the leak mechanism remains.

Appendix — Installation of the PL-259 to LMR-400 Coax Cable

The integrity of the connection of the PL-259 to the coax is critical to this experiment. The technique for installing connectors is described here.

Requirement 1

Ensure that each PL-259 connector is soldered to the coax braid at all four solder holes, as well as at the center conductor to the center pin to ensure electrical stability.

Requirement 2

Ensure each of the four solder holes and the center pin of the PL-259, are soldered shut to prevent the possibility of water entry here, even though the PL-259 might leak elsewhere.

LMR-400 was used due to the cable construction. It has an aluminum foil on top of the dielectric and underneath the factory-tinned braid. While this provides (nearly) 100% electrical shielding, there is a bonus. The process of soldering the braid to the barrel often involves considerable heat to be applied for some time to induce solder flow between the barrel and braid. Without foil to contain dielectric melt, the dielectric will ooze up through the braid, fouling the solder connection. In many cases the braid is not even tight to the barrel, and little to no heat transfer takes place, and so the connection is either fouled or incomplete, or both. The four small solder holes fill with solder quickly without any confirmation that the braid underneath has actually picked up solder. The solution to these problems is to cut open a slot between any two adjacent holes with a Dremel ® tool equipped with a cut-off disk, see Figure A.

Tin the LMR factory-tinned braid with a little more solder. Screw the connector on to the coax and watch the braid pass by the slot and become fully engaged on the coax cable. Clamp and hold the coax steady in a vise.

Take a hot, tinned soldering iron of considerable thermal mass and place the tip in the slot, heating both the barrel and the tinned braid at the same time. Start feeding solder. Very soon solder will flow on both the braid and the barrel. You can visually verify the connectivity.

While the assembly is hot, go to the two remaining holes, insert the tip of the iron into the hole and feed in solder, which will wick in to the hole almost immediately. Visually inspect the solder joint. The benefits of this procedure are (1) visual verification of the solder joints, and (2) containment of dielectric melt compromising the joint due to the foil.

While hot, the center pin must be wiped clean with a rag down to the original diameter of the center pin, or be filed down when cold, to ensure the connection from the PL-259 to either an SO-239 or female to female barrel is smooth and with no distortions.

John White, VA7JW, earned the Canadian Basic license, VE7AAL in 1959 and upgraded to Advanced in 1960. He attended technical high school in Victoria BC, 1957 through 1960, then enrolled in Victoria University in 1960. One year later, he enrolled in Engineering University of British Columbia (UBC) in Vancouver, and graduated as Electrical Engineer in 1965. He achieved Professional Engineer (P.Eng) status in 1968. His working career includes GTE, Lenkurt Electric, Glenayre, and Norsat. John remained an active HF ham throughout. He belongs to the Victoria Short Wave Club, VE7EZ, North Shore Amateur Radio Club, VE7NSR, and Orca DX and Contest Club, VA7ODX. John has published technical articles in The Canadian Amateur, (TCA), QST and QEX.

Notes

[1]View forward and reflected waves resulting in a standing wave at, **https://en.wikipedia.org/wiki/File:Standing_wave_2.gif**.

[2]For the relationship between SWR, RL, Power, Losses see, **radio.feld.cvut.cz/personal/mate-jka/download/VSWR%20table.pdf table**.

[3]Scotch Super 88® Electrical Tape, **solutions.3mcanada.ca/wps/portal/3M/en_CA/CA-Electrical/Home/Solutions/Mining/?PC_Z7_RJH9U5230GG7802DQ1VSFM1ON4000000_nid=GS6VLXWVB0gsS8HLFF93PWgIKMCP5CD39Xbl**.

[4]Self-Vulcanizing Fusion Tape #122, **www.plym-outhrubber.com/wp-content/uploads/2015/02/catalogous_plymouth.pdf**.

[5]See STUF®, **www.crossdevices.com/**.

[6]See PacCoax Seal®, **coaxseal.com**.

Signal to Noise Ratio and Polarization at HF Considering Atmospheric Noise

The Report 47[1] referenced by Robert Sternowski, WBØLBI in his "Polarization in HF Atmospheric Noise" article[2] compares noise received by vertically and horizontally polarized antennas. However, what actually interests us as amateurs is (1) what polarization is best for transmitting, and (2) what polarization is best for receiving since the transmitting and receiving processes may not be symmetrical. While we can easily compute the signal strength versus height and polarization by considering a coherent interference between a direct wave and a ground-reflected wave[3, 4], the same does not necessarily hold for noise, which sums up non-coherently.

Using the method of Siwiak, we compare a horizontally polarized dipole 23 feet above a medium ground, with ground-mounted 21-ft tall vertically polarized antenna at the 2.3, 5, and 10 MHz frequencies of Hagn's study. We found that for signal reception, a low horizontally polarized dipole is at a disadvantage compared with the ground mounted vertical. The calculation was in "receive" but by reciprocity, is also true in transmit, so it suggests that one should transmit on vertical polarization in MF and low HF, at least as compared to a low horizontal dipole.

This suggests that at the 2.3 MHz frequency of the Hagn study, and at 23 feet and higher, a Waller Flag, for example, should be horizontally polarized, but your ground-mounted transmitting antenna should be vertically polarized. The ionosphere will rotate the polarizations, so one need not worry about cross polarization. The story repeats, but is less pronounced for 5 MHz. At 10 MHz there is almost no SNR advantage to using a dipole at 23 ft compared with a vertical. That might change for a higher antenna; we just do not have the data.

Hagn and Barker[5] wrote their final report in 1970, and reported the ratio of signal-plus-noise to noise, (S+N)/N, on "HF-expedient antennas". They might have as easily said Field Day antennas! They compared a ground mounted λ/4 vertical, a 30° slant wire, a 5:1 inverted L and a λ/2 dipole at a height of λ/8. Quoting Hagn and Barker,

"The dipole exhibited the greatest (S + N)/N. The average (S+N)/N on the slant wire typically was 2 to 4 dB below that on the dipole, whereas the inverted L was typically 6 to 8 dB worse than the dipole. As expected, the (S + N)/N on the monopole was significantly lower — about 26 dB — below the dipole. The noise picked up by the inverted L was typically only about 0.5 dB greater than the dipole noise, whereas the noise on the slant wire and monopole was typically 2 to 3 dB greater than the dipole noise. Evidently the difference in signal gain was more important than the noise pickup in determining the difference in (S + N)/N."

"Information on the signal-plus-noise (and interference) to noise (and interference) ratio on a path of this length may be inferred from the 50-mile data obtained during the HF manpack tests over varied terrain during sunspot minimum (RM 3). ***These results at 3.6 MHz for the 15 W HC-162 (AN/PRC-74) indicated roughly a 20% chance of communication with whips, a 50% chance with 30° slant wires, and a 75% chance with λ/2 dipoles at λ/10 above ground-during any 24-hour period.****"* [The emphasis is ours.]

Of course all of this is based on a single set of noise measurements made decades ago at a location closer to our Florida antipode than to us! — *Best regards, Ed Callaway, N4II and Kai Siwiak, KE4PT*.

Notes

[1] G. Hagn, R.Chindahporn and J. Yarborough, "HF Atmospheric Radio Noise on Horizontal Dipole Antennas in Thailand", Special Technical Report 47, Stanford Research Institute, Jun., 1968. DTIC accession number AD681879; **www.dtic.mil/dtic/tr/fulltext/u2/681879.pdf**.

[2] R. Sternowski, WBØLBI, "Polarization in HF Atmospheric Noise", *QEX* May/Jun 2017, pp 26-27.

[3] K. Siwiak, KE4PT, "Is There an Optimum Height for an HF Antenna?", *QST*, Jun 2011, pp 33-36.

[4] K. Siwiak, KE4PT, "An Optimum Height for an Elevated HF Antenna", *QEX,* May/Jun 2011, pp 32-38.

[5] G. H. Hagn and G. E. Barker, "Research Engineering and Support for Tropical Communications", Final Report, Project 4240, Stanford Research Institute, Feb. 1970. DTIC accession number AD889169; **www.dtic.mil/get-tr-doc/pdf?AD=AD0889169.**

Send your short *QEX* Technical Note to the Editor, via e-mail to qex@arrl.org. We reserve the right to edit your letter for clarity, and to fit in the available page space. "*QEX* Technical Note" may also appear in other ARRL media. The publishers of *QEX* assume no responsibilities for statements made by correspondents.

Letters to the Editor

Polarization in HF Atmospheric Noise, (May/Jun 2017)

Dear Robert,

Did the Special Technical Report 47 take into account the difference in received energy based on radiation lobes of the antennas? How much of this effect is the angle of arrival of the noise source, vs. the actual polarization of the noise itself? I guess that the reader wants to know what kind of antenna will result in a better SNR rather than where the noise comes from. Does Report 47 mention what the noise source was they were measuring?

I'm curious how this sort of measurement changes with man-made sources vs. natural sources. Do you have any data on that? Thanks again for the article, I really enjoyed it. — *73, Mark Smith, KC7CJ*, **mark@halibut.com**.

[The author replies],

I'm glad that you enjoyed the article. You ask some good questions. (1) They used electrically small antennas, so that antenna pattern lobes are non-existent. (2) They did this in a rural area in Thailand, away from manmade noise. There was no attempt at directionality of sources, since thunderstorms come from all directions. (3) They measured noise power with calibrated instruments, not SNR. (4) Your question about manmade noise is a classic question. Generally speaking, E-field man-made noise appears to be vertically polarized [near the ground.— *Ed.*]. With horizontally polarized signals, the electric lines of force parallel to the ground tend to be "shorted" by the ground. Vertically polarized waves can travel along the ground surface.— *Cheers, Bob Sternowski, WBØLBI.*

Dear Bob,

Oh, that's very interesting. I hadn't thought about the physics of what happens to horizontal and vertical waves near the ground. — *73, Mark Smith, KC7CJ*

[This topic continues in a *QEX* Technical Note that describes the signal to noise behavior of vertically and horizontally polarized antennas. Noise is not necessarily coherent, but the physics of coherent waves near ground is shown in, K. Siwiak, KE4PT, "An Optimum Height for an Elevated HF Antenna", *QEX*, May/Jun 2011 pp 32-38, and especially in Figures 5 and 6.— *Ed.]*

Experiments with a Broadband, High-Dynamic Range, Low Noise HF Receiver Preamplifier, (Jul/Aug 2017)

Dear Editor,

I was very glad to see my HF receiver preamplifier article appear in print. *QEX* readers may find it helpful to know that CR1 is a 1N5818 Schottky diode, CR2 is a 1N4005 or similar, and that the materials cost was about US$60. — *73, Scott Roleson, KC7CJ*.

Dear Scott,

In a pair of hard-to-find articles for *RF Design Magazine* (February and March 1996) titled "A Tutorial on Intermodulation Distortion" and "Practical Steps for Accurate Computer Simulation", I specifically used my own optimized design of the Norton-Podell lossless feedback amplifier with a 1:5:3 ratio transformer. I showed how to accurately model the transistor and the parasitics of all of the important components including the transformer. The amplifier covered 5 to 80 MHz. The simulations included parasitics, but not losses, and predicted a gain of 8.9 dB with a measured gain of 8.74 dB. I built a number of them and used two different transistors. The NEC NE46134 produced a measured 3rd order intercept (IP3) of +48.8 dBm. I also tried the NE85634 and its measured IP3 was +47.5 dBm. The IP3 of the simulation and measurements agreed within one decibel — the accuracy of the HP lab spectrum analyzer. These IP3 results were obtained with one transistor, not two in push-pull as Makhinson had done. — *73, Jeffrey Pawlan, WA6KBL,* **pawlan@ieee.org**.

[The author replies],

Indeed, the articles are hard to find. I wonder if there might be some way to resurrect them for *QEX*? Thanks for this insight. I find it interesting that your more complete circuit analysis provided results that more closely matched measured gain. As I was working on this project, I often thought that there must be more to this circuit than what the equations in the original patent showed, given that most experimenters seemed to find a large discrepancy between theoretical and actual gain. Double good reason to get your earlier work back into print, I think. *— Best regards, Scott Roleson, KC7CJ*.

Send your *QEX* Letters to the Editor to, ARRL, 225 Main St., Newington, CT 06111, or by fax at 860-594-0259, or via e-mail to qex@arrl.org. We reserve the right to edit your letter for clarity, and to fit in the available page space. "Letters to the Editor" may also appear in other ARRL media. The publishers of *QEX* assume no responsibilities for statements made by correspondents.

Upcoming Conferences

36th Annual ARRL and TAPR Digital Communications Conference

Saint Louis, Missouri,
September 15 – 17, 2017
Holiday Inn Airport West
www.tapr.org

Mark your calendar and start making plans to attend the premier technical conference of the year, the 36th Annual ARRL and TAPR Digital Communications Conference to be held September 15 – 17, 2017 in Saint Louis, MO.

Conference presentations, meetings, and seminars will be held at the Holiday Inn Airport West, 3400 Rider Trail South, Earth City, MO 63045, 314-291-6800.

The ARRL and TAPR Digital Communications Conference is an international forum for radio amateurs to meet, publish their work, and present new ideas and techniques. Presenters and attendees will have the opportunity to exchange ideas and learn about recent hardware and software advances, theories, experimental results, and practical applications.

Topics include, but are not limited to: Software Defined Radio (SDR), digital voice, digital satellite communications, Global Position System (GPS), precision timing, Automatic Packet Reporting System(tm)(APRS), short messaging (a mode of APRS), Digital Signal Processing (DSP), HF digital modes, Internet interoperability with Amateur Radio networks, spread spectrum, IEEE 802.11 and other Part 15 license-exempt systems adaptable for Amateur Radio, using TCP/IP networking over Amateur Radio, mesh and peer to peer wireless networking, emergency and Homeland Defense backup digital communications, using Linux in Amateur Radio, updates on AX.25 and other wireless networking protocols.

Mid-Atlantic VHF Conference

Bensalem, Pennsylvania,
October 6 – 8, 2017
Holiday Inn Bensalem-Philadelphia
www.packratvhf.com/latest.htm#Anchor-49575

Sponsored by the Mt. Airy VHF Club (Pack Rats). Conference topics include VHF, UHF and microwave construction, operating, digital modes, EME, antennas, roving and more. Additional speakers and Proceedings papers sought. Contact **rick1ds@hotmail.com**.

The conference will be held at the Holiday Inn Bensalem-Philadelphia, 327 Street Rd. (Rt. 132), Bensalem, PA 19020, 215-639-9100.

See website for conference updates and registration details.

23rd Annual Pacific Northwest VHF-UHF-Microwave Conference

Moses Lake, WA,
October 13 – 15, 2017
Best Western Lake Front
www.pnwvhfs.org

Join other weak-signal VHF, UHF and Microwave operators for the 23rd Annual PNW VHF Society Conference!

The conference will be held at Best Western Lake Front Hotel, 3000 Marina Dr., Moses Lake, WA 98837, 509-765-9211

Call for Papers: The Pacific Northwest VHF Society is looking for speakers and papers for our next conference.

Please send your abstract to Jim K7ND, **secretary@pnwvhfs.org**. Authors will be notified of acceptance by September 14 for inclusion in the program and it will be posted on the website.

Abstracts are solicited on these VHF-UHF-Microwave topics and more: MSK441 and other digital modes; propagation; microwaves; EME Tools, tips and techniques; frequency stabilization; hilltopping, roving and portable operation; antenna theory and design; the world above 1000 MHz; operating with satellites; transverters and amplifiers; software defined radio; remote station operation; amateur television; contest equipment, techniques and strategy; lasers and other radiation sources; and other subjects related to VHF and up.

See website for details.

Microwave Update 2017

Santa Clara, California,
October 26 – 29, 2017
Biltmore Hotel
www.microwaveupdate.org

Microwave Update (MUD) is an international conference dedicated to microwave equipment design, construction, and operation. It is focused on, but not limited to, amateur radio on the microwave bands. The 50 MHz and Up Group of Northern California is pleased to host this year's event. The conference will be held at the Biltmore Hotel, 2151 Laurelwood Road, Santa Clara, California 95054.

Call for Presentations and Papers: The program committee is calling for papers and presentations on the technical and operational aspects of microwave amateur radio communications. Tell us about your latest project, design or operating adventures. Please e-mail your proposals, questions and submissions to **mud2017.papers@gmail.com**. Don't wait until the beginning of September to let us know what you're planning!

Presentations selected for the technical program may be given in person or by proxy. Please send an abstract and expected duration no later than **September 5, 2017** so that we can determine and announce the program agenda the following week. Ideally, send your draft presentation by the same date. We encourage presenters to submit a companion paper for publication in the proceedings book. This paper would ideally be text based and expand on the presentation slides, but a simple copy of the slides is also okay. Either way, this material must be received no later than **September 12, 2017** to be included in the book. Additional material (presentation slides, schematics, source code, more text, background info, etc.) to be included on the proceedings CD must arrive no later than **October 8, 2017.** All conference attendees will receive a copy of the book and CD.

Full details, including suggested topics, paper guidelines, schedule, and hotel information can be found on their website.

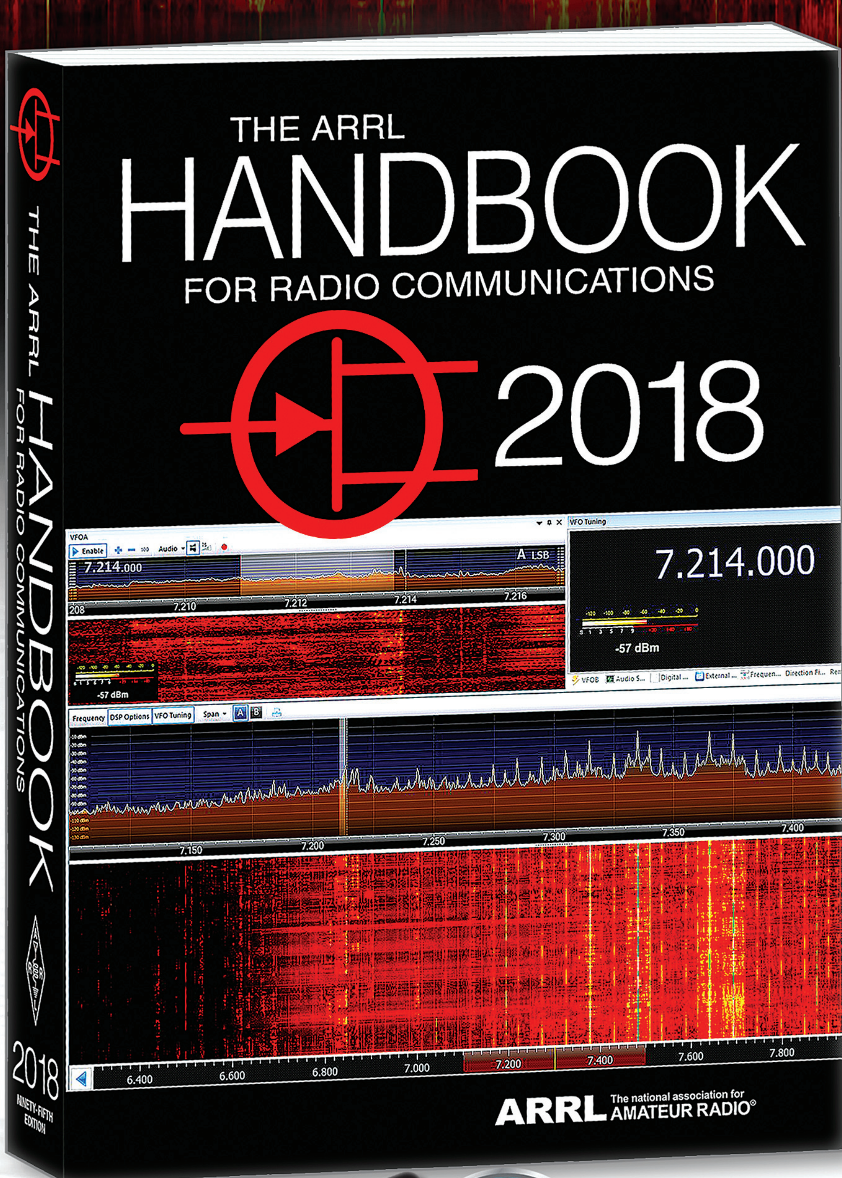

Major NEW Edition!

The ARRL Handbook is the most widely used one-stop reference and guide to radio technology principles and practices. This fully revised 2018 edition has been extensively updated, and includes new content on **Software Defined Radio** (**SDR**) and **Signal Processing** (**DSP**), **Grounding and Bonding**, **Solar Cycle 24-25**, **Tower Safety**, and **Building Remote-Control Stations**.

New Projects

- VHF/UHF/Microwave Filters and Transmission Lines
- Software-Controlled and Manual Preselectors for 1.8-30 MHz
- Digital Mode Audio-Based VOX/PTT Interface
- PICAXE-Based Timer
- Arduino-Based CW IDer
- 6-Meter Halo Antenna
- Big Wheel VHF/UHF Mobile Antenna
- Off-Center End-Fed Portable 40-6 Meter Antenna
- Crossed-Dipole Omnidirectional Antenna for 1296 MHz
- Spudgun Antenna Launcher
- CW Reception Filter

Shipping in October!

BONUS OFFER! First Ever ARRL Member Call Sign Badge— FREE when you pre-order the **Hardcover** edition by September 30, 2017 Member Badge is laser engraved with your name and call sign. Includes magnetic fastener and slot for bulldog clip. Offer limited to online orders placed with ARRL.

2018 ARRL Handbook Hardcover and BONUS Member Badge
ARRL Item No. 0727
Only $59.95

2018 ARRL Handbook Softcover
ARRL Item No. 0710
Only $49.95

ARRL The national association for AMATEUR RADIO®

www.arrl.org/shop
Toll-Free US 888-277-5289, or elsewhere +1-860-594-0355

The Handbook is available from ARRL and ARRL Publication Dealers everywhere!

hear and be heard

MAXIMIZE YOUR COMMUNICATIONS CAPABILITIES

SteppIR Antenna Systems are designed for performance, period. From amateur to advance, stationary to portable, our antennas and accessories take you to the next level of capability. Whether it's a basic 2-Element 20-6 or a DreamBeam DB18, there is nothing that can match a SteppIR.

YAGI ANTENNAS - The best performing HF antennas available

VERTICAL ANTENNAS - True quarter wave continuous coverage

PORTABLE ANTENNAS - Full legal limit power handling capability for DXpeditions

MOBILE AND FIXED TOWERS - We'll help you configure a Tower/Antenna Package

ACCESSORIES - Our long list of the best accessories completes your antenna package

FEATURED PRODUCT

CrankIR

CrankIR is a high-performance on-the-road antenna. Perfect for deploying your team in an emergency, or for a public service event. CrankIR sets up quickly and allows you the flexibility to change bands even faster. Just "Turn the Crank", that's it! No fussing with changing traps, taps, or coils. This is a serious antenna for every communication need – even if your "emergency" is just letting fellow hams know its a beautiful day on the beach!

steppIR
ANTENNA SYSTEMS

www.steppir.com 425-453-1910